



Cite this: *React. Chem. Eng.*, 2026, **11**, 562

## Homogeneous catalysis in liquid organic hydrogen carriers: advances, challenges, and future directions

Juliana Mana Edor, \*<sup>a</sup> Gershon Amenuvor,<sup>b</sup>  
 Phillimon Modisha <sup>a</sup> and Dmitri Bessarabov<sup>a</sup>

Liquid organic hydrogen carriers (LOHCs) offer a promising solution for safe, efficient, and reversible hydrogen storage and transport. While heterogeneous catalysts have traditionally dominated LOHC hydrogenation and dehydrogenation, homogeneous catalysts present distinct advantages, including high selectivity, tunable active sites, and operation under milder conditions. This review systematically examines recent advances in the design and application of homogeneous catalysts for the hydrogenation and dehydrogenation of both homocyclic LOHCs, such as benzene, toluene, and naphthalene derivatives, and N-heterocyclic LOHCs, including quinolines, carbazoles, and indoles. Emphasis is placed on structure–activity relationships, mechanistic insights, and emerging trends, with a focus on catalysts based on both noble and earth-abundant metals. Beyond catalyst performance, we address key challenges in homogeneous catalyst recovery, recycling, and process integration, all of which are critical for industrial scalability. By identifying current gaps in the literature and outlining future research priorities, this work aims to guide the development of efficient, reversible, and economically viable homogeneous catalytic systems for next-generation hydrogen storage technologies.

Received 7th November 2025,  
 Accepted 15th February 2026

DOI: 10.1039/d5re00486a

[rsc.li/reaction-engineering](https://rsc.li/reaction-engineering)

### 1. Introduction

Hydrogen is valued for its high gravimetric energy density and is a promising candidate for clean and sustainable energy. It can be generated from water using renewable

<sup>a</sup> HySA Infrastructure Centre of Competence, Faculty of Engineering, North-West University, Private Bag X6001, Potchefstroom, 2531, South Africa. E-mail: 36967432@mynwu.ac.za

<sup>b</sup> Department of Chemistry, Kwame Nkrumah University of Science and Technology, Kumasi, Ghana



**Juliana Mana Edor**

*Dr. Juliana Mana Edor is a Postdoctoral Research Fellow at Hydrogen South Africa (HySA Infrastructure Centre of Competence), North-West University, where her research focuses on developing efficient catalysts for the (de)hydrogenation of liquid organic hydrogen carriers (LOHCs). She holds a PhD in Chemistry from North-West University and an MSc with distinction from the University of Johannesburg. Her expertise lies in organometallic chemistry, homogeneous catalysis, and sustainable hydrogen technologies, with multiple peer-reviewed publications in international journals. She is a recipient of the prestigious OWSD PhD fellowship and Schlumberger Foundation Faculty for the Future Fellowship.*



**Gershon Amenuvor**

*Dr. Gershon Amenuvor is a Coordination and Organometallic Chemist with a strong research focus on mixed-donor ligand metal complexes and their applications in homogeneous catalysis and metallodrug discovery. He is currently a Lecturer at the Kwame Nkrumah University of Science and Technology, Ghana. Gershon earned his BSc (Hons) from KNUST and his MSc and PhD from the University of Johannesburg under the supervision of Prof. James Darkwa and Dr. Banothile C.E. Makhubela. Passionate about teaching and mentorship, his research spans synthesis and catalysis, and the development of bioactive compounds for tackling tropical diseases.*



energy sources such as solar or wind power in regions with abundant energy and then transported to areas lacking sufficient energy generation. However, hydrogen's low energy density by volume in the gaseous state remains a major challenge regarding its storage and transportation.<sup>1</sup>

Researchers have been investigating various hydrogen storage options to overcome these challenges.<sup>2–7</sup> Options include the use of inorganic chemical hydrides, metal–organic frameworks, and metal hydrides to develop efficient and safe storage solutions that facilitate the transportation of hydrogen from energy-rich areas to places where it can be used effectively, thereby promoting a sustainable hydrogen economy.<sup>8</sup>

Due to their numerous advantages, liquid organic hydrogen carriers (LOHCs) have gained attention as a highly promising solution for hydrogen storage/release and transportation technology.<sup>9–12</sup> LOHC systems consist of organic compounds that ideally allow for the bidirectional storage/release of hydrogen through catalytic (de)hydrogenation approaches while retaining their molecular integrity across numerous storage cycles. To be technically viable, LOHCs should also possess a viable range of chemical and physical characteristics, which include low melting points, thermal stability, advantageous (de)hydrogenation kinetics and thermodynamics, broad large-scale accessibility, and low toxicity.<sup>13</sup>

Since their conceptual introduction in the 1970s, with systems such as the toluene–methylcyclohexane pair, LOHCs have demonstrated practical applications, including large-scale demonstrations like Chiyoda Corporation's SPERA Hydrogen™ technology.<sup>14</sup> Benzyltoluene (BT), developed through collaboration between FAU Erlangen–Nürnberg and adopted by Hydrogenious Technologies, also exemplifies a commercially viable LOHC owing to its high hydrogen storage capacity (HSC) and stability.<sup>15</sup> Such successes

highlight their potential for facilitating hydrogen transport over long distances.<sup>1,14,15</sup> However, challenges remain, including concerns about toxicity, high energy demand for dehydrogenation, and the need for further advancements in catalyst efficiency.<sup>16</sup> This review provides an overview of recent progress in homogeneous catalysis for the (de)hydrogenation of LOHCs, with particular emphasis on homocyclic and N-heterocyclic systems. Homogeneous catalysts, particularly those based on platinum group metals (PGMs) like Ru, Ir, and Rh, and earth-abundant metals like Co and Ni, offer high selectivity and activity under mild conditions for the (de)hydrogenation of certain LOHCs. Even though challenges such as catalyst separation, high costs, and limited scalability hinder industrial adoption, their high selectivity and low temperature requirements make them suitable for systems that operate at low temperatures. Homogeneous catalysts often remain dissolved in the LOHC, requiring energy-intensive separation methods like distillation. However, advanced techniques such as biphasic systems and nanofiltration, discussed in section 6, provide less energy-demanding alternatives. While several reviews have covered heterogeneous catalysts in LOHC systems,<sup>17,18</sup> fewer have explored the nuances of homogeneous catalysis.<sup>19–21</sup> This review uniquely examines the role of ligand design, metal–ligand cooperativity, and precious and non-precious metal catalysts in improving catalytic efficiency for LOHC applications. Rather than presenting a full techno-economic analysis, this review also discusses key techno-economic descriptors that govern the practical deployment of aromatic and heteroaromatic LOHC systems, with emphasis on catalyst performance, operating conditions, and system-level constraints. In addition, some major industrial applications of homogeneous catalysis and various strategies for homogeneous catalyst recovery and reuse are discussed briefly. By analyzing the advances in catalyst design,



**Phillimon Modisha**

*Dr. Phillimon Modisha joined HySA Infrastructure in 2014 as a research engineer, where he supports key HySA projects, particularly in liquid organic hydrogen carrier (LOHC) technology. He has developed strong first-hand expertise in LOHC systems through extensive collaborative research and continues to train students in this field. He obtained his PhD in Chemical Engineering from North-West University in 2021*

*under the supervision of Prof. Dmitri Bessarabov. Now an Associate Professor in the Faculty of Engineering, his research focuses on liquid organic hydrogen storage at the HySA Infrastructure Centre of Competence.*



**Dmitri Bessarabov**

*Dmitri Bessarabov is a Professor at North-West University, South Africa, and Director of the HySA Infrastructure CoC under the Department of Science, Technology, and Innovation. An expert in hydrogen energy and electrochemical technologies, his research spans PEM water electrolysis, renewable hydrogen production, storage, and refuelling systems. He has held senior R&D roles at Aker Kvaerner Chemetics, Ballard*

*Power Systems, and AFCC in Canada. Dmitri has co-authored over 200 scientific publications and leads the South African–Japanese SATREPS programme in green hydrogen and ammonia research.*



mechanistic insights, and the sustainability of LOHC systems, we aim to provide an overview that is comprehensive in the field while identifying challenges and future directions for research.

## 2. Overview of LOHC systems

While LOHCs have proven effective for hydrogen storage, understanding the differences between the various systems is critical for optimizing their performance. Several organic compounds have the potential to be used as LOHCs. These include simple compounds such as formic acid (FA), methanol, liquefied ammonia, and amino alcohols.<sup>22</sup> In addition, LOHC media based on functional groups such as amides and imides, often operating *via* metal–ligand cooperative pincer catalysts, have been reported and are discussed extensively in the literature.<sup>23,24</sup> These systems generally operate under comparatively mild temperature conditions.

Other LOHC candidates are based on homocyclic and heterocyclic aromatic compounds, such as methylcyclohexane, decalin, perhydrocarbazole, and indoline, which typically require higher operating temperatures for hydrogen release. For LOHC-based hydrogen storage systems intended for mobile or vehicle-integrated applications, the operating temperature of the hydrogen release step represents a critical design constraint. Many vehicular platforms cannot accommodate the high temperatures (>250–300 °C) required for the dehydrogenation of several established aromatic LOHCs due to limitations associated with heat management, system complexity, start-up time, and catalyst durability. Examples include perhydrobenzyltoluene, employed by Hydrogenious Technologies,<sup>15</sup> which operates under high dehydrogenation temperatures. Consequently, non-aromatic LOHC media that enable hydrogen release at lower temperatures (<200 °C) have attracted increasing attention for temperature-sensitive applications.<sup>25,26</sup> These considerations highlight the importance of matching LOHC thermodynamics and kinetics with application-specific temperature constraints, particularly for mobile systems where high-temperature operation is impractical.

However, the present review focuses specifically on aromatic homocyclic and heterocyclic LOHC systems, which constitute a distinct class of hydrogen carriers with unique hydrogenation–dehydrogenation mechanisms, thermodynamic profiles, and catalyst requirements. The following sections, therefore, examines these aromatic systems and their key properties.

### 2.1. Homocyclic LOHCs

Homocyclic hydrocarbons are considered the simplest prospects for LOHCs due to the smooth transformation between hydrogenated alicyclic and dehydrogenated aromatic compounds.<sup>27,28</sup> Systems such as cyclohexane–benzene,<sup>29–31</sup> methylcyclohexane–toluene,<sup>32–34</sup> and decalin–naphthalene<sup>35–38</sup> pairs have been studied as examples because of their wide industrial prevalence, commercial accessibility, and relatively low toxicity. In recent times, systems utilizing diphenylmethane,<sup>39,40</sup> BT,<sup>41–43</sup> dibenzyltoluene (DBT),<sup>10,11,44,45</sup> and biphenyl<sup>46–48</sup> have been examined as well. The primary benefit of using cyclic hydrocarbons as LOHCs is their ability to supply CO<sub>x</sub>-free hydrogen. Another notable feature is their high hydrogen weight-specific energy density, ranging from 6–8 wt%. Additionally, due to their low melting and high boiling points, they are well-suited for the storage and transport of hydrogen from centralized production sites to refuelling facilities. A low melting point and a high boiling point are essential for a potential LOHC to ensure the substance retains its liquid state across a broad temperature range. This facilitates convenient hydrogen storage and transport by preventing solidification at low temperatures and excessive vaporization at high temperatures, ensuring both practicality and safety.<sup>49</sup> Table 1 illustrates the properties of various homocyclic compounds as potential LOHCs, while Fig. 1 shows the structures of selected homocyclic LOHCs.

### 2.2. Heterocyclic LOHCs

The dehydrogenation of cyclic hydrocarbons to form homocyclic aromatics is an attractive process for hydrogen release but faces limitations due to its inherent endothermic nature. This reaction typically requires high dehydrogenation enthalpies (~64–69 kJ mol<sup>-1</sup> of H<sub>2</sub>) compared to the

**Table 1** Important physicochemical properties to consider in the (de)hydrogenation of selected homocyclic LOHC pairs (L = liquid state; S = solid state)

Properties of selected homocyclic LOHC pairs

Homocyclic aromatic LOHC system	State	Melting point (°C)	Boiling point (°C)	Enthalpy (kJ mol <sup>-1</sup> H <sub>2</sub> )	Hydrogen storage capacity (wt%)	References
Benzene/cyclohexane	L/L	5.5/	80	54.0	7.2	16, 41, 52
Toluene/methylcyclohexane	L/L	-95/-127	111/101	57.5	6.2	16, 31, 41, 52
Naphthalene/decalin	S/L	80	218	61.9	7.3	16, 41, 20
Dibenzyltoluene/perhydrodibenzyltoluene	L/L	-39/-34	390	61.5	6.2	20, 53
Benzyltoluene/perhydrobenzyltoluene	L/L	-30	280	64	6.25	20
Diphenylmethane/dicyclohexylmethane	L/L	26/-19	265/248–250	—	6.7	31
Biphenyl/bicyclohexyl	S/L	69–71/3–4	254–255/238	—	7.3	31, 52



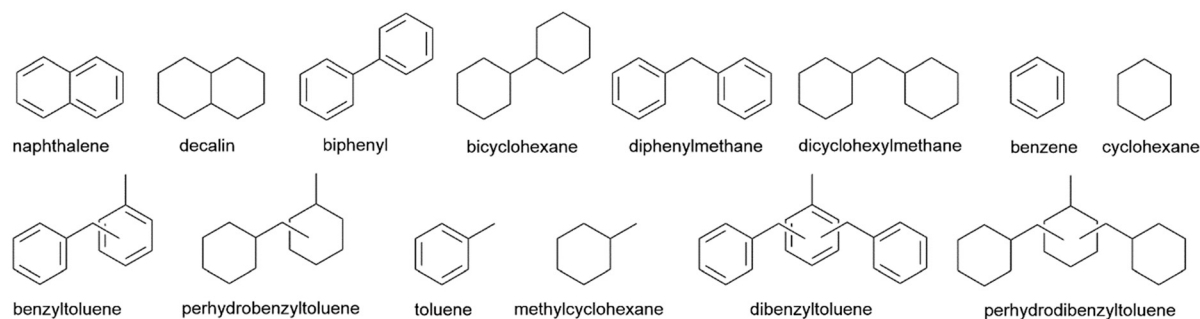


Fig. 1 Structures of selected homocyclic LOHC pairs.

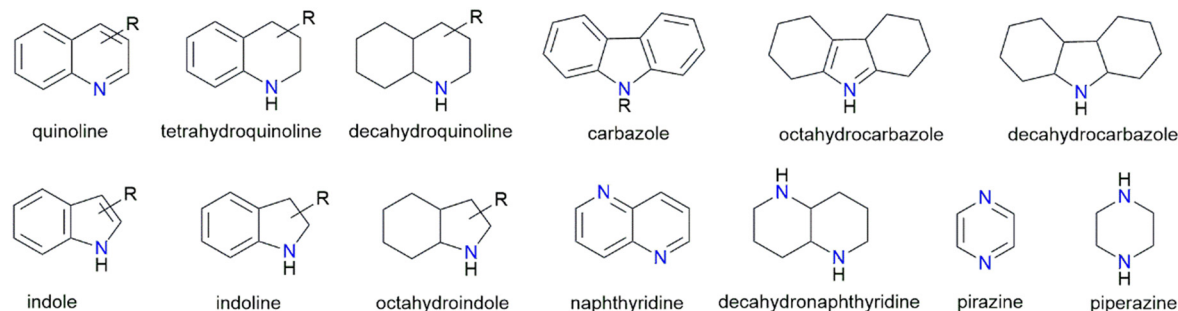


Fig. 2 Structures of selected heterocyclic LOHCs.

exothermic and readily achievable hydrogenation of aromatic hydrocarbons.<sup>50</sup> This difference in energy requirements significantly impacts the feasibility of using homogeneous catalysts, as they can operate at relatively low temperatures while overcoming the high energy barrier.<sup>28</sup> Meanwhile, introducing heteroatoms into the aromatic ring system offers a potential avenue for overcoming the limitations of dehydrogenation.

Studies by Pez and coworkers<sup>51</sup> suggest that incorporating heteroatoms results in a considerable loss of aromaticity upon dehydrogenation, thereby lowering the enthalpy of dehydrogenation. This opens doors for exploring dehydrogenation reactions with heterocyclic substrates using homogeneous catalysts. Following this, research interest in the catalyzed (de)hydrogenation of

N-heterocycles was focused on molecules such as carbazoles, quinolines, and indoles.<sup>20</sup> Their advantages include the ease of reversibility, easier H<sub>2</sub> release than from alicyclics, favorable kinetic and thermodynamic properties, and low vapor pressure. Furthermore, they contain only the widely available elements C, H, and N. Fig. 2 shows the structures of selected heterocyclic LOHCs, and Table 2 presents the properties of various heterocyclic compounds useful as potential LOHCs.

Both homocyclic and heterocyclic LOHC systems rely heavily on efficient catalysis to facilitate reversible hydrogen storage. Homogeneous catalysis is an emerging and powerful approach for enhancing the performance of these systems, as discussed in the sections that follow.

Table 2 Important physicochemical properties to consider in the (de)hydrogenation of selected N-heterocycle LOHC pairs (L = liquid state; S = solid state)

N-Heterocyclic LOHC system	State	Melting point (°C)	Boiling point (°C)	Enthalpy (kJ mol <sup>-1</sup> H <sub>2</sub> )	Hydrogen storage capacity (wt%)	References
Perhydro- <i>N</i> -ethylcarbazole/ <i>N</i> -ethylcarbazole	L/S	-85/69	261/355	54.0	5.80	16, 52, 54
<i>N</i> -Phenylcarbazole		91-93		57.5	6.94	20
Decahydroquinoline/quinoline	L/L	37/-15	214/252	61.9	7.18	54
Tetrahydroquinoline/quinoline	L/L	9-14/-15	249/252	61.9	3	18
Decahydroquinoline/dine/quinoline	L/L	-23/-2	232/271	64	6.58	54
1-Methylperhydroindole/1-methylindole	L/S	-25/-20	230/239	51.9	5.76	54, 61
2,6-Dimethyldecahydro-1,5-naphthyridine/2,6-Dimethyl-1,5-naphthyridine	S/S	—	—	—	5.94	52
Pyrazine/piperazine	S/S	52/106	115/146	—	5.3	144



### 3. Advances in homogeneously catalyzed de(hydrogenation) of homocyclic LOHCs

Aromatic hydrogenation typically requires more stringent conditions than in the case of nonaromatic unsaturated bonds. While heterogeneous catalysts have proven effective for LOHC-relevant aromatic hydrogenation systems, homogeneous metal complex catalysts remain relatively less studied, specifically in the field of LOHC technology for hydrogen storage. Heterogeneous catalysts benefit from increased surface area and support properties, such as Lewis acidity or Brønsted basicity. Additionally, heterogeneous catalysis is advantageous due to its ease of separation, which reduces operating costs and makes it widely used in industry. However, its drawbacks include limited activity and selectivity.<sup>55</sup> In contrast, homogeneous catalysts can be optimized through careful ligand design to enhance their catalytic activity.<sup>21,30</sup> Homogeneous catalysis, though less common in industrial applications due to the challenging and costly catalyst separation, offers superior selectivity and higher activity and eliminates mass transfer limitations, potentially enabling lower operating temperatures.<sup>55</sup>

#### 3.1. Hydrogenation of homocyclic aromatics with catalysts based on platinum group metals

Boxwell *et al.*<sup>29</sup> in 2002 designed a system using catalyst 1 ( $[\text{Ru}(p\text{-cymene})(\eta^2\text{-TRIPHOS})\text{Cl}][\text{PF}_6]$ ), where  $\text{TRIPHOS} =$

1,1,1-tris(diphenylphosphinomethyl)ethane illustrated in Fig. 3, for hydrogenating arenes in dichloromethane (DCM) and ionic liquid. The system is effective in catalyzing the hydrogenation of toluene and benzene (90 °C, 61 bar  $\text{H}_2$  pressure, 1 h) to afford the corresponding cyclohexane, with turnover frequency (TOF) values of 205  $\text{h}^{-1}$  and 476  $\text{h}^{-1}$ , respectively. The catalyst showed high activity in both ionic liquids and DCM, with significantly higher activity in ionic liquids. Unlike in DCM, where it decomposes, no considerable activity loss was observed after five runs in ionic liquids. Several allylbenzenes were also hydrogenated with this system. Particularly, the availability of a free phosphine is relevant for selectivity towards arene hydrogenation; otherwise, the hydrogenation does not occur.

Rojas' group<sup>56</sup> devised the hydrogenation of various aromatics with a homogeneous Ru-based catalyst. The catalyst  $[\text{Ru}(\eta^5\text{-C}_5\text{H}_5)\text{Cl}(\text{TPPDS})_2]$  (2) (TPPDS:  $\text{P}(\text{C}_6\text{H}_5)(\text{C}_6\text{H}_4\text{SO}_3)_2$ ) reduced toluene, benzene, and *m*-xylene in a biphasic (*n*-heptane/water) medium to the corresponding cyclohexane analogues. Toluene, *m*-xylene, and benzene, generated products in yields of 80%, 25%, and 43%, respectively, after 4 h reaction time (105 °C, 96 bar  $\text{H}_2$ , and substrate/catalyst ratio 600 : 1). The activity increased with  $\text{H}_2$  pressure, temperature, pH, and ionic strength. Furthermore, the aqueous catalytic system can undergo several cycles with little reduction in activity.<sup>56</sup> Water-soluble Ru complexes 3–5 were analyzed in the hydrogenation of arenes. Complexes 3 and 5 exhibited similar TOF values, with 3 being more active

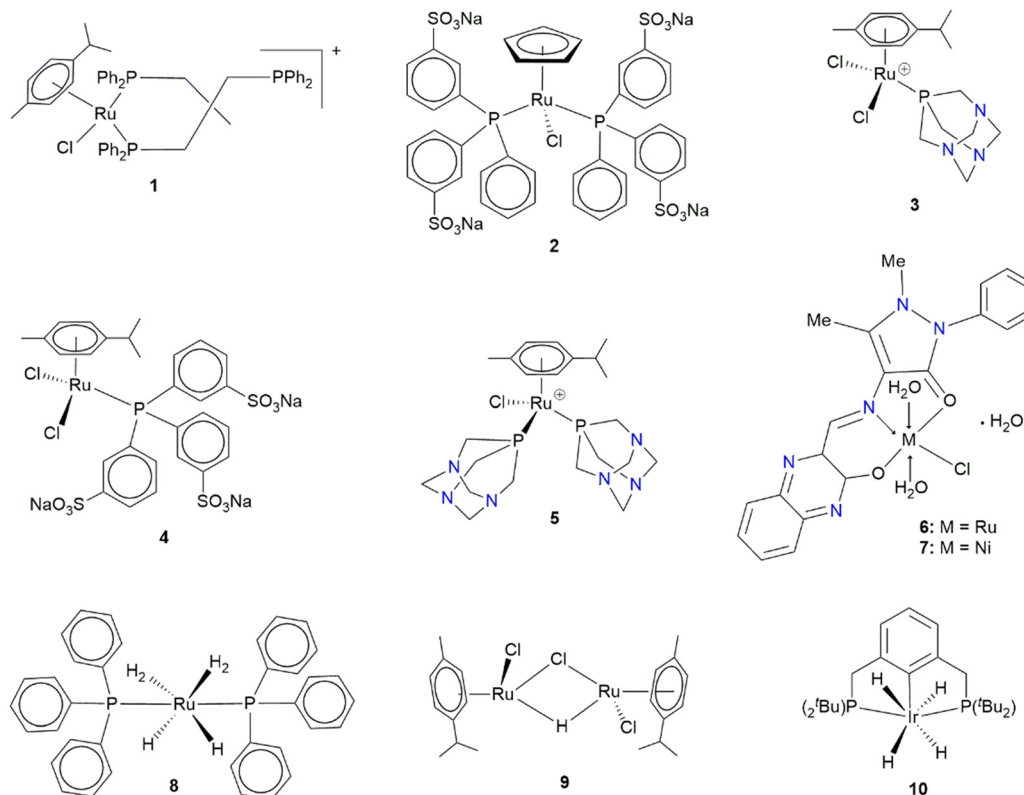


Fig. 3 Examples of molecular catalysts based on PGMs for (de)hydrogenating aromatic LOHCs.



than 5 while complex 4 was significantly more active than complexes 3 and 5. The presence of mercury had little impact on the activity of 3 and 5. However, adding mercury to the reaction medium with 4 resulted in a considerable reduction in turnover number, indicating the decomposition of 4 to form catalytically active colloidal species.<sup>57</sup> Arun *et al.*<sup>30</sup> used 3-hydroxyquinoline-2-carboxalidene-4-aminoantipyrine (L)-coordinated Ru complex (6) in the hydrogenation of benzene to produce a mixture of cyclohexadiene and cyclohexane in 18% and 82% yields, respectively (Scheme 1). A TOF of 5372 h<sup>-1</sup> was recorded in reducing benzene (80 °C, 50 bar H<sub>2</sub> pressure, 3.64 × 10<sup>-6</sup> mol catalyst, and 0.34 mol benzene). Mercury drop tests confirmed a homogeneously catalyzed process. Under identical reaction conditions, the Ru complex (6) gave a superior conversion with a TOF of 5372 h<sup>-1</sup>, while the nickel catalyst (7) gave a lower conversion with a TOF of 1718 h<sup>-1</sup>.

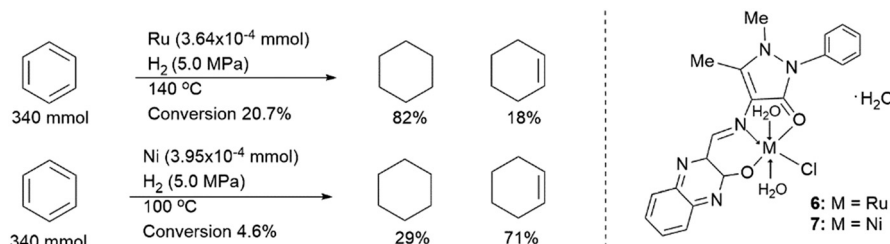
In 2010, Vangelis *et al.*<sup>31</sup> showed that the Rh/TPPTS-catalyzed (TPPTS: triphenylphosphine trisulfonate) hydrogenation of benzene exhibits remarkably high catalytic performance (TOF > 204 000 h<sup>-1</sup>), producing cyclohexane quantitatively in an organic/aqueous biphasic system (130 °C, 80 bar H<sub>2</sub> pressure, 5 min). The catalyst was readily recycled by employing phase separation techniques. Recycling experiments showed consistently high catalytic activities over five consecutive runs. Borowski *et al.*<sup>58</sup> successfully partially hydrogenated anthracene under mild conditions (3 bar H<sub>2</sub> pressure, 80 °C) using the homogeneous bis(dihydrogen) Ru complex 8. The reaction selectively hydrogenated the terminal aromatic rings, yielding a mixture of 4*H*-anthracene and 8*H*-anthracene. Hydrogenation of the first ring was significantly faster than the second. However, prolonged reaction times resulted in catalyst decomposition and metal precipitation, preventing complete conversion to the 8*H*-anthracene. Chatterjee *et al.*<sup>59</sup> utilized a dinuclear monohydrido-bridged ligand complexed to Ru[(η<sup>6</sup>-*p*-cymene)RuCl]<sub>2</sub>(μ-H-μ-Cl) (9), demonstrating exceptional efficiency and selectivity in the hydrogenation of diverse arenes and heteroarenes. The complete hydrogenation of various arenes (including benzene, toluene, naphthalene, and anthracene) to the generated cycloalkanes was achieved in high yields using 1 mol% catalyst loading (90 °C, 50 bar H<sub>2</sub>, 40 h). However, further analysis revealed that the arenes are hydrogenated by *in situ*-generated Ru NPs.

### 3.2. Catalysts based on earth-abundant metals

Muetterties and Hirsekorn<sup>60</sup> in 1974, developed the tris(phosphite) cobalt allyl complex 11 (Fig. 4), employed in homogeneous arene hydrogenation. Under mild conditions, hydrogenation of arenes was observed, tolerating mesitylene, xylene, and naphthalene, and resulting in *cis*-cycloalkanes in all instances. At 25 °C, benzene hydrogenation to cyclohexane occurred at a slow rate, with approximately 20 catalyst cycles completed in 48 h. A comprehensive mechanistic analysis suggested that the *cis* selectivity stemmed from consecutive *syn* additions of a Co-allyl hydride over the arene's C-C bonds, followed by the reduction of the diene and olefin products, thus indicating homogeneous catalysis.<sup>61</sup> Rothwell<sup>62</sup> has shown that Nb and Ta complexes with sterically shielded alkoxide ligands are efficient precatalysts in the all-*cis* arene hydrogenations.

The tantalum trihydride complex 12 could be separated and utilized directly, whereas the phosphine-free niobium counterpart was generally produced *in situ* through hydrogenolysis of the tribenzyl-ligated precursor.<sup>62</sup>

A Mo-catalyzed arene hydrogenation method was developed by Joannou *et al.*<sup>63</sup> in 2018. The pyridine(diimine) Mo catalyst [(4-<sup>t</sup>Bu-<sup>i</sup>PrPDI)Mo(CH<sub>2</sub>SiMe<sub>3</sub>)<sub>2</sub>] (<sup>i</sup>PrPDI: 2,6-(2,6-(C(CH<sub>3</sub>)<sub>2</sub>H)<sub>2</sub>C<sub>6</sub>H<sub>3</sub>N=CMe)<sub>2</sub>C<sub>5</sub>H<sub>3</sub>N) 13 was able to hydrogenate benzene and several substituted arenes, employing a 5 mol% catalyst loading at 60 °C, 4 bar of H<sub>2</sub>, and 24 h, demonstrating that the barrier to hydrogenating arenes can be greatly reduced by transition metal complexes. Then Hierlmeier *et al.*<sup>64</sup> investigated Mo cyclohexadienyl complexes [(PIP)Mo(COD)] (PIP: phosphino(imino)pyridine, COD: 1,5-cyclooctadiene) 14–16 in the hydrogenation of benzene. Cyclohexane was produced using 0.18 mol% catalyst loading (at 23 °C, and 6.89 bar H<sub>2</sub> pressure). Scheme 2 illustrates the suggested catalytic cycle. When using the iso-propyl-substituted variant 16, a turnover number (TON) of 56 was obtained. This was a significant improvement over the previously reported system [(4-<sup>t</sup>Bu-<sup>i</sup>PrPDI)Mo(CH<sub>2</sub>SiMe<sub>3</sub>)<sub>2</sub>],<sup>63</sup> which had a TON of 19 at 23 °C. The system also catalyzed the hydrogenation of toluene to form methylcyclohexane at 4 bar H<sub>2</sub> pressure. The development of the above Mo catalysts demonstrates that, in homogeneous arene hydrogenation, an arene incorporation into the metal-hydride bond proceeds with a relatively minimal kinetic barrier when using Mo phosphino(imino)



Scheme 1 Benzene hydrogenation catalyzed by Schiff base-coordinated Ru and Ni complexes.<sup>21,30</sup>



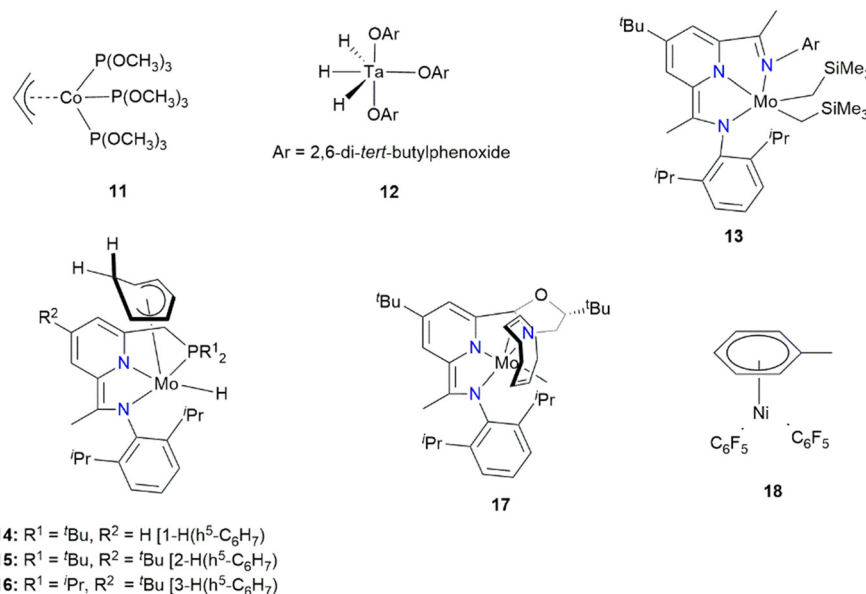
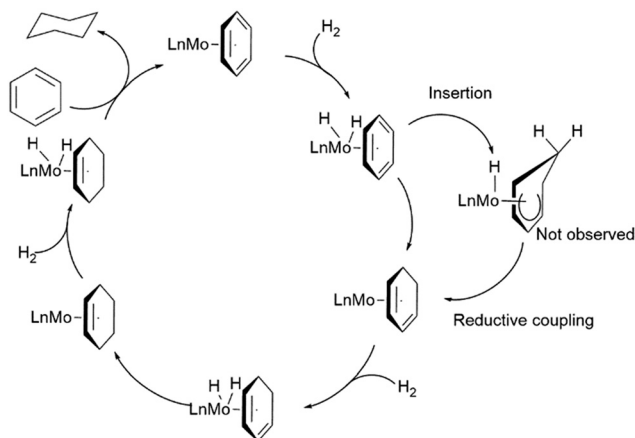


Fig. 4 Selected earth-abundant metal catalysts for hydrogenating homocyclic LOHCS.



Scheme 2 Proposed mechanism for the Mo-catalysed arene hydrogenation.<sup>64</sup>

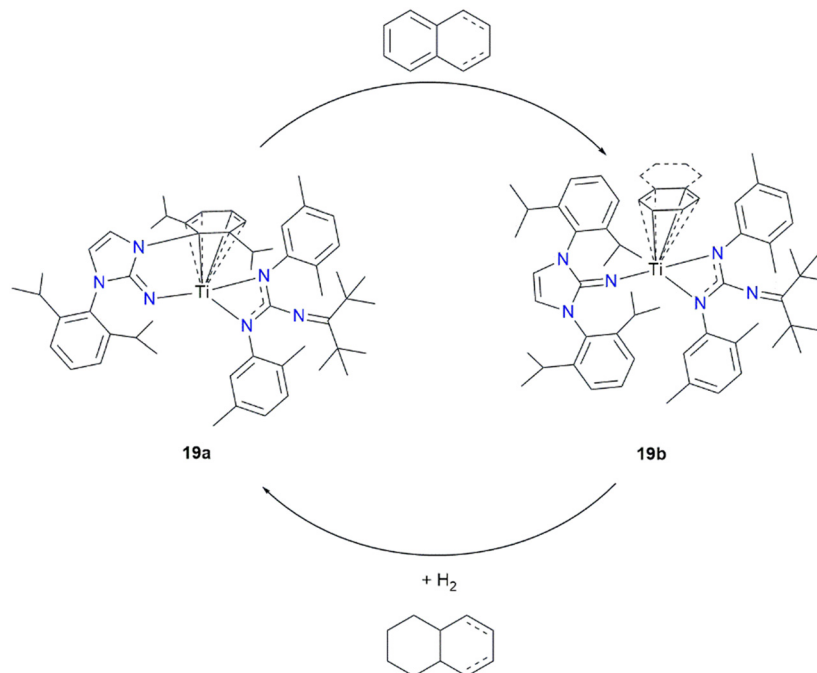
pyridine complexes.<sup>64</sup> The first step begins with the  $\eta^6$ -binding of the arene, after which the dihydrogen undergoes oxidative addition to the metal. Then, inserting the arene's C(sp<sup>2</sup>)-C(sp<sup>2</sup>) bond into a metal hydride bond results in the formation of a cyclohexadiene complex, followed by reductive elimination. Subsequent hydrogenations proceed similarly through oxidative addition, insertion, and reductive elimination steps to afford the cycloalkane. Furthermore, a similar approach, commencing with the dihydride Mo complex, is conceivable.<sup>64</sup> Viereck *et al.*<sup>65</sup> also demonstrated the hydrogenation of naphthalene derivatives using enantioenriched Mo complex **17**, [4-<sup>t</sup>Bu-(<sup>t</sup>BuOIP)Mo(COD)] (OIP: oxazoline imino(pyridine)). Results indicated that hydrogenating the various substrates (eight examples) produced the corresponding decalin in yields ranging between 45 and 95% with enantioselectivities up to 95% ee.

Klabunde *et al.*<sup>66</sup> reported that the  $\eta^6$ -nickel(II) catalyst **18** reduces toluene to methylcyclohexane under high H<sub>2</sub> pressure (101 bar) at 25 °C. However, the complex showed signs of decomposition, forming C<sub>6</sub>F<sub>5</sub>H and inactive Ni(0) species; hence, the observed TONs were limited to  $\leq 10$ . A Ti(IV)-guanidine complex (**19**) was used in the hydrogenation of various poly and monocyclic aromatics. The substrates (toluene-d<sub>8</sub>, benzene-d<sub>6</sub>, anthracene, and naphthalene) were reduced to afford the corresponding cyclohexanes at 80 °C under very low H<sub>2</sub> pressure. NMR data (<sup>1</sup>H, <sup>2</sup>H, and <sup>13</sup>C NMR) suggested that the Ti catalyst **19a** was converted to Ti catalyst **19b**, which is the active species when H<sub>2</sub> is introduced, as illustrated in Scheme 3.<sup>67</sup>

In 2019, Zeng and coworkers<sup>68</sup> reported the regiocontrolled polycyclic hydrocarbons hydrogenation with Cr and Co catalysts at ambient temperature for the first time. Using CrCl<sub>3</sub> and MeMgBr with diamino ligands in THF, only one terminal benzene ring of anthracene was selectively hydrogenated at 50 bar H<sub>2</sub> pressure. In contrast, when Co(acac)<sub>3</sub> was used, both terminal benzene rings in the anthracene framework were hydrogenated when using isopropanol and MeMgBr at ambient temperature (RT) in THF, under 80 bar H<sub>2</sub>. The proposed mechanism involves low-valent metal species as active catalysts that undergo migratory insertion into the C=C bond of anthracene, forming an intermediate that is subsequently hydrogenated, and the active species is regenerated.

Johnson *et al.*<sup>69</sup> in 2025 reported benzene hydrogenation utilizing early transition metal catalyst precursors. Diverse precursors, including transition metal complexes of groups 4 and 5, were investigated for benzene hydrogenation. For group 4, homoleptic -CH<sub>2</sub><sup>t</sup>Bu complexes, [M(CH<sub>2</sub><sup>t</sup>Bu)<sub>4</sub>] (M = Ti, Zr, Hf), were selected, while group 5 catalysts were based on -CH<sub>2</sub>SiMe<sub>3</sub> ligands, specifically [V(CH<sub>2</sub>SiMe<sub>3</sub>)<sub>3</sub>(THF)] and





**Scheme 3** Interconversion between titanium catalysts **19a** and **19b**.<sup>67</sup>

$[M_2(\mu_2\text{-CSiMe}_3)_2(\text{CH}_2\text{SiMe}_3)_4]$  ( $M = \text{Nb, Ta}$ ). In all cases,  $^1\text{H}$  NMR spectroscopy confirmed cyclohexane as the sole product after catalysis. The results illustrated that employing milder reaction conditions ( $120\text{ }^\circ\text{C}$ , *ca.* 27 bar  $\text{H}_2$ ), groups 4 and 5 transition metal complexes are active catalysts in hydrogenating benzene. The most active catalysts were Nb- and Hf-based, achieving initial TOF values of 1055 and 1155 mol  $\text{C}_6\text{H}_6$  mol  $\text{M}^{-1}$  h $^{-1}$ , respectively. Remarkably, under identical reaction conditions, these TOFs exceed those achieved with conventional heterogeneous catalysts, such as RANEY® Ni and 5 wt% Pd/C, thus highlighting the potential of group 4 and 5 metal complexes as effective alternatives for use in benzene hydrogenation.

### 3.3. Reversible hydrogenation of aromatic LOHCs using homogeneous catalysts

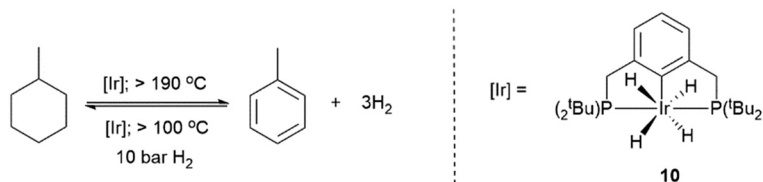
Ir pincer complex **10** was demonstrated in homogeneous catalysis by Jensen for hydrogen storage/release in aromatic hydrocarbons.<sup>70,71</sup> Complex **10** showed activity for the reversible hydrogenation of the methylcyclohexane/toluene pair (Scheme 4). The oxidation reaction proceeded inside a reaction chamber fitted with a tubular membrane enabling

selective  $\text{H}_2$  gas permeation at  $190\text{ }^\circ\text{C}$ . The hydrogenation also proceeded in the same flask at 10 bar  $\text{H}_2$  pressure and  $>100\text{ }^\circ\text{C}$ . Table 3 provides a summary of catalysts discussed for the homogeneous hydrogenation of homocyclic LOHCs.

## 4. Advances in homogeneously catalyzed (de)hydrogenation of N-heterocyclic compounds

### 4.1. Quinolines

The quinoline moiety (Fig. 5) is an attractive candidate for LOHCs. Quinolines are liquid at ambient conditions, with high boiling and melting points as outlined in Table 4.<sup>20,72</sup> Quinolines are primarily derived from fossil oil processing, wood preservation, or can be synthetically produced from anilines.<sup>20</sup> Quinoline derivatives are also found in many natural products, particularly quinoline-based alkaloids.<sup>73</sup> Although the HSC of quinolines is very high, the high dehydrogenation enthalpy of  $61.9\text{ kJ mol}^{-1}$ ,<sup>74</sup> moderate toxicity ( $\text{LD}_{50} = 460\text{ mg kg}^{-1}$ ), and potential adverse effects on organisms across various trophic levels and food chains<sup>75</sup> limit their widespread application in LOHC technology.<sup>20</sup>



**Scheme 4** Reversible hydrogenation of toluene/methylcyclohexane with Ir complex **10**.



**Table 3** Summary of catalysts used for the homogeneous hydrogenation of homocyclic LOHCs (as discussed above) and key metrics

Catalyst	Substrate/product	Conv. (%)	Selectivity (%)	TON	TOF (h <sup>-1</sup> )
[Ru( <i>p</i> -cymene)(η <sup>2</sup> -TRIPHOS)Cl][PF <sub>6</sub> ]	Benzene/cyclohexane				476
	Toluene/methylcyclohexane				205
[Ru(η <sup>5</sup> -C <sub>5</sub> H <sub>5</sub> )Cl(TPPDS) <sub>2</sub> ]	Benzene/cyclohexane	43			
	Toluene/methylcyclohexane	80			
[Ru(η <sup>6</sup> -C <sub>10</sub> H <sub>14</sub> )(pta)Cl <sub>2</sub> ]	Benzene/cyclohexane			170	
	Toluene/methylcyclohexane			130	
[Ru(η <sup>6</sup> -C <sub>10</sub> H <sub>14</sub> )(TPPTS)Cl <sub>2</sub> ]	Benzene/cyclohexane			488	
	Toluene/methylcyclohexane			365	
[Ru(η <sup>6</sup> -C <sub>10</sub> H <sub>14</sub> )(pta) <sub>2</sub> Cl] <sup>+</sup>	Benzene/cyclohexane			150	
	Toluene/methylcyclohexane			129	
[Ru <sup>II</sup> (3-hydroxyquinoxaline-2-carboxalidene-4-aminoantipyrine)(Cl)(H <sub>2</sub> O) <sub>2</sub> ]-H <sub>2</sub> O	Benzene/cyclohexane	20.7	82	—	5372
[RuH <sub>2</sub> (η <sup>2</sup> -H <sub>2</sub> ) <sub>2</sub> {P(C <sub>6</sub> H <sub>11</sub> ) <sub>3</sub> }] <sub>2</sub>	Anthracene	100	4H anth = 99.3	0.3	
			8H anth = 0.7	50	
[(η <sup>6</sup> - <i>p</i> -Cymene)RuCl] <sub>2</sub> (μ-H-μ-Cl)	Benzene/cyclohexane		90	150	
	Toluene/methylcyclohexane		90		
	Naphthalene/decalin		>99		
	Anthracene/tetradecahydroanthracene		40		
RhCl <sub>3</sub> ·3H <sub>2</sub> O/TPPTS	Benzene/cyclohexane	57	100		204
					400
[Ni <sup>II</sup> (3-hydroxyquinoxaline-2-carboxalidene-4-aminoantipyrine)(Cl)(H <sub>2</sub> O) <sub>2</sub> ]-H <sub>2</sub> O	Benzene/cyclohexane	5.5	31		1718
(4- <sup>t</sup> Bu- <sup>i</sup> Pr <sup>+</sup> PDI)Mo(CH <sub>2</sub> SiMe <sub>3</sub> ) <sub>2</sub>	Benzene/cyclohexane	98		19	
[(PIP)Mo(COD)]	Benzene/cyclohexane			56	
4- <sup>t</sup> Bu- <sup>t</sup> Bu <sup>+</sup> OIP)Mo(COD)	Naphthalenes/decalins		45–95%		
[η <sup>6</sup> -Toluenebis-(pentafluorophenyl)nickel(II)]	Toluene/methylcyclohexane			≤10	
[(η <sup>6</sup> -Im <sup>Dip</sup> P <sup>N</sup> ) <sup>(xyket)guan</sup> Ti]	Benzene-d <sub>6</sub> /cyclohexane-d <sub>6</sub>			1	0.05
	Toluene-d <sub>8</sub> /methylcyclohexane-d <sub>8</sub>			1.8	0.09
	Naphthalene/tetralin			4.4	0.22
	Anthracene/octahydroanthracene			4.6	0.23
[Ti(CH <sub>2</sub> <sup>t</sup> Bu) <sub>4</sub> ]	Benzene	23			173
[Zr(CH <sub>2</sub> <sup>t</sup> Bu) <sub>4</sub> ]	Benzene	97			691
[Hf(CH <sub>2</sub> <sup>t</sup> Bu) <sub>4</sub> ]	Benzene	96			1155
[V(CH <sub>2</sub> SiMe <sub>3</sub> ) <sub>3</sub> (THF)]	Benzene	0			0
[Nb <sub>2</sub> (μ <sub>2</sub> -CSiMe <sub>3</sub> ) <sub>2</sub> (CH <sub>2</sub> SiMe <sub>3</sub> ) <sub>4</sub> ]	Benzene	98			1055
[Ta <sub>2</sub> (μ <sub>2</sub> -CSiMe <sub>3</sub> ) <sub>2</sub> (CH <sub>2</sub> SiMe <sub>3</sub> ) <sub>4</sub> ]	Benzene	44			177

**Fig. 5** Structures of selected quinolines used as LOHCs.**Table 4** Properties of selected quinoline derivatives<sup>20,72</sup>

Quinoline derivative	State	Melting point (°C)	Boiling point (°C)	HSC (wt%)
Quinoline	Liquid	-40	238	7.2
2-Methylquinoline	Liquid	-9	247.6	6.6
Isoquinoline	Liquid	27	243.3	7.2

**4.1.1.1. Catalysts for hydrogenation of quinolines.** A range of homogeneous catalysts has been investigated for quinoline hydrogenation, utilizing earth-abundant and precious metal complexes. Methods such as direct and transfer hydrogenation (TH) have been applied to quinolines. The subsequent sections describe the catalysts implemented in these methods.

**4.1.1.1. Direct hydrogenation.** Pressurized H<sub>2</sub> gas is required for direct hydrogenation, necessitating complex high-pressure equipment. Despite this, direct hydrogenation offers benefits such as high efficiency, yielding products of high purity, and easy scalability for industrial use.<sup>75</sup> Various earth-abundant metal complexes have been employed to hydrogenate quinolines and other N-heterocycles directly (Fig. 6). For instance, an efficient cobalt catalyst for hydrogenating a diverse group of compounds was designed by Duan *et al.*<sup>76</sup> utilizing the moisture and air-stable, scalable complex (20), which is easily activated by potassium hydroxide. Quinolines bearing different groups were quantitatively hydrogenated effortlessly using 0.1 mol% catalyst loading and 10 mol% KOH in <sup>i</sup>PrOH under 30 bar H<sub>2</sub> at 100 °C for 48 h. The half-sandwich [WCl(η<sup>5</sup>-Cp)(CO)<sub>3</sub>] complex (21) was explored for the homogeneous reduction of quinolines using pressurized H<sub>2</sub> gas.<sup>77</sup> Applying 2 mol% catalyst loading in <sup>i</sup>PrOH, under high H<sub>2</sub> pressure (50 bar), afforded 94% tetrahydroquinoline (THQ) in 14 h. Bench-stable nickel complexes with metallated tripodal ligands (22) efficiently hydrogenated quinoline quantitatively to THQ with



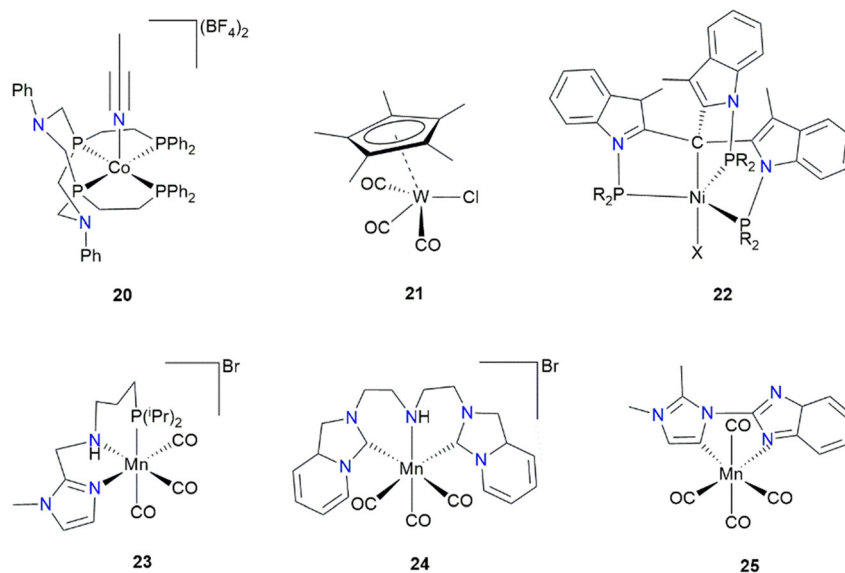


Fig. 6 Catalysts reported for the direct hydrogenation of quinolines.

a catalyst loading of 2.5 mol% in toluene under 10 bar  $H_2$  at 30 °C for 15 h.<sup>78</sup> Papa *et al.*<sup>79</sup> reported room temperature N-heterocycle hydrogenation catalysis using NNP-Mn(i) pincer complex (23).

At 20 bar  $H_2$  pressure, catalyst loading of 2.5 mol%, and 10 mol% of  $KO^tBu$  in THF, hydrogenating various quinolines resulted in excellent conversions. Relative to the earlier results reported by employing  $MnCO_3Br$  as a catalyst, it was revealed that complex 23 was superior in hydrogenating quinolines with substituents at positions 5 and 8.<sup>79</sup> Kumar *et al.*<sup>80</sup> designed a bis-NHC-armed  $CN^H C$ -Mn pincer catalyst (24), hydrogenating heteroarenes efficiently. In particular, quinoline was hydrogenated to 1,2,3,4-THQ in 97% yield using 2 mol% catalyst loading, 20 mol%  $KO^tBu$  under 60 bar  $H_2$  pressure, and 120 °C for 12 h. The group also reported a mesoionic carbene-Mn(i) complex (25) in N-heteroarene hydrogenation. However, only 20% product yield was achieved when quinoline was reduced under the optimum reaction conditions.<sup>81</sup>

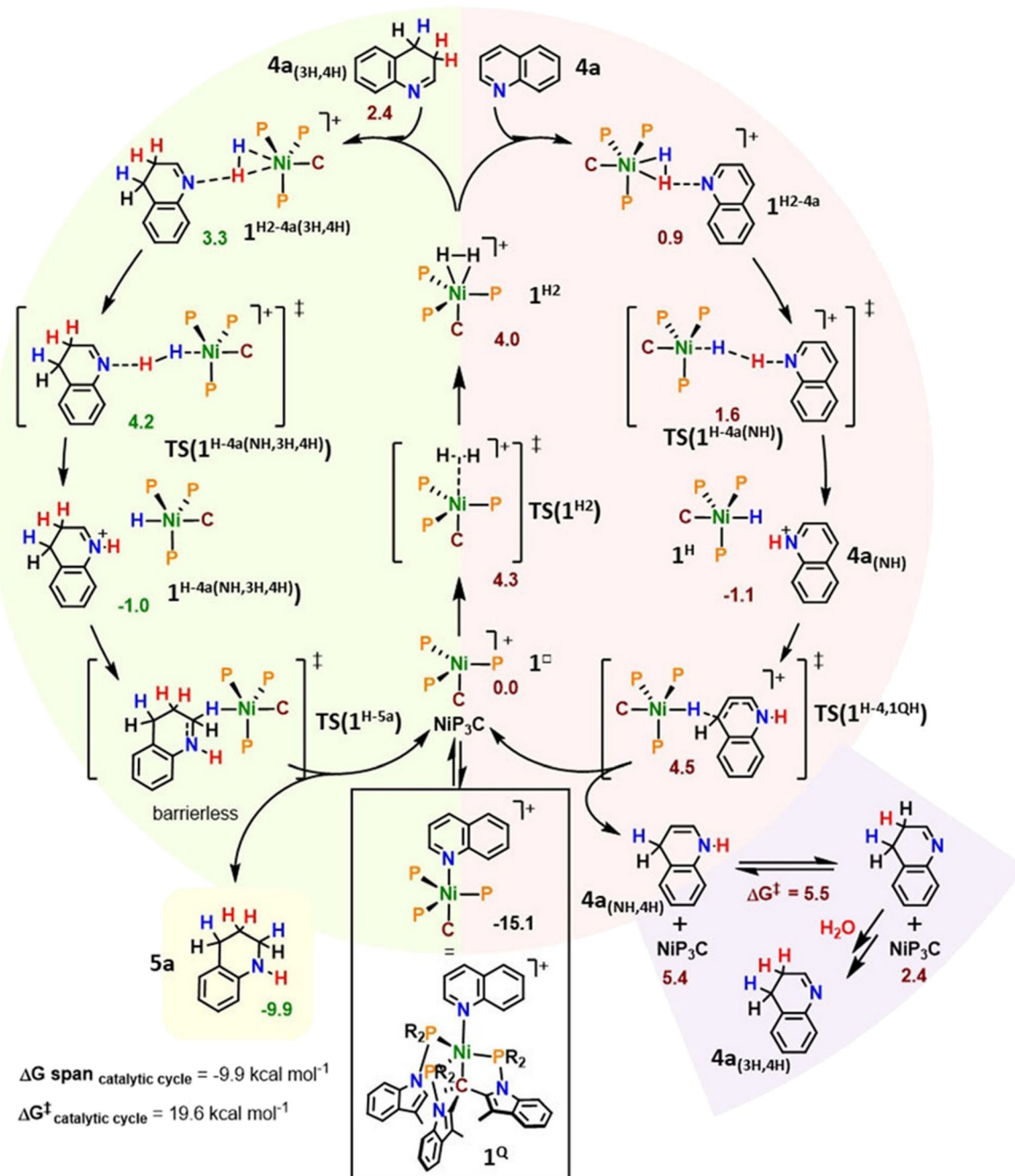
**4.1.1.2. Mechanistic studies.** In efforts to further understand the mechanism, Michaliszyn *et al.*<sup>78</sup> employed DFT methods (B3LYP/6-31g\*) with a focus on the heterolytic activation route of  $H_2$  as illustrated in Scheme 5. The initial intermediate, Ni-quinoline adduct ( $1^Q$ ), is 15.1 kcal·mol<sup>-1</sup> more stable than the decoordinated complex ( $1^\square$ ). Coordination of  $H_2$  to  $1^\square$  forms  $1^{H_2}$  ( $\Delta G = 19.1$  kcal mol<sup>-1</sup> from  $1^Q$ ) through a low-energy transition state, yielding a highly labile  $\eta^2-H_2$  complex. Notably,  $\eta^2-H_2$  coordination elongates the *trans* Ni-C bond by 0.037 Å, similar to the effect of quinoline coordination (0.045 Å). The oxidative addition of  $H_2$  to Ni(II) was ruled out due to a high activation barrier ( $\Delta G^\ddagger = 33.4$  kcal mol<sup>-1</sup>). Instead, heterolytic  $H_2$  activation is facilitated by quinoline. The formation of the  $1^{H_2-4a}$  adduct stabilizes  $1^{H_2}$  ( $\Delta G = -3.1$  kcal mol<sup>-1</sup>), followed by a low-energy transition state ( $\Delta G^\ddagger = 0.7$  kcal mol<sup>-1</sup>), resembling frustrated

Lewis pair behavior, where Ni acts as a Lewis acid and quinoline as a base. This results in exergonic H-H bond cleavage, weakening the Ni-C bond *via trans* effect (elongation 0.076 Å). Molecular orbital analysis reveals that  $H_2$  destabilizes the Ni-C bond in  $1^{H_2}$ , with its LUMO (Ni  $d_{z^2}$ ) resembling that of  $1NTf_2$ , where  $NTf_2$  is weakly coordinating. The  $1^{H_2-4a}$  adduct stabilizes the Ni-C bond through C-Ni-H interaction, showcasing the electronic flexibility of Ni. Following heterolytic cleavage, the protonated quinoline ( $4a_{(NH)}$ ) undergoes nucleophilic attack by Ni(II)-H at position 4 ( $\Delta G^\ddagger = 5.6$  kcal mol<sup>-1</sup>; overall barrier = 19.6 kcal mol<sup>-1</sup>), yielding  $4a_{(NH,4H)}$ . A rapid isomerization equilibrium with  $4a_{(3H,4H)}$  ( $\Delta G^\ddagger = 5.5$  kcal·mol<sup>-1</sup>) aligns with previous reports and deuteration experiments.<sup>82</sup> Finally,  $4a_{(3H,4H)}$  undergoes heterolytic  $H_2$  activation to form  $4a_{(NH,3H,4H)}$ , followed by a barrierless Ni(II)-H attack at position 2, yielding the final product ( $5a$ ).<sup>78</sup>

**4.1.1.3. Transfer hydrogenation.** Transfer hydrogenation (TH) refers to the process of adding hydrogen to a molecule using an alternative source of hydrogen instead of molecular hydrogen, as it offers a practical and efficient way to produce various hydrogenated substances. This method serves as a useful alternative to DH. TH has recently attracted significant attention in hydrogenation research. The advantages of TH include (i) the absence of hazardous pressurized  $H_2$  gas and complex experimental setups, (ii) its availability and low cost, and the ease of handling the hydrogen donors, (iii) recyclability of the main byproduct, and (iv) ease of access to and the stability of the catalysts used.<sup>83</sup> TH offers a straightforward and viable substitute for traditional hydrogenation methods and eliminates the need for high-pressure apparatus or gas handling.<sup>84</sup>

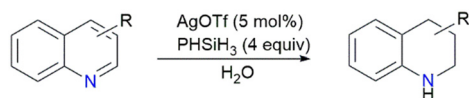
**4.1.1.3.1. Using silanes as a hydrogen source.** Bi and coworkers<sup>85</sup> reported an effective silver catalyst in reducing electron-deficient N-heteroarenes and quinolines in aqueous





**Scheme 5** Proposed catalytic cycle. Red values show initial quinoline hydrogenation yielding  $4a_{(NH,4H)}$  and isomerizing to  $4a_{(3H,4H)}$ . Green values relate to the reduction of  $4a_{(3H,4H)}$  to  $5a$ <sup>78</sup> (image reproduced with permission from John Wiley & Sons, Inc., all rights reserved).

medium with hydrosilanes, as illustrated in Scheme 6. They reported that in just 10 min, 2-methylquinoline was reduced to the 1,2,3,4-THQ derivative in 98% yield at RT. The system enhances quinoline reduction in the absence of both a base



**Scheme 6** Transfer hydrogenation of quinolines using silane as the hydrogen source.

and a ligand and performs under modest conditions. Similarly, in 2022, the  $[\text{Ir}(\text{COD})\text{Cl}]_2$ -catalyzed TH of various quinolines was performed using hydrosilane as the hydrogen source in methanol without any external ligand or base. The system allowed for the scalable synthesis of the 1,2,3,4-THQ core moiety under mild conditions.<sup>86</sup>

**4.1.1.3.2. Using FA as a source of hydrogen.** In 1984, Watanabe *et al.*<sup>87</sup> reported the TH of quinolines using dichlorotris(triphenylphosphine) Ru complex with FA acting as a hydrogen transfer agent. The reactions were achieved using stoichiometric amounts of FA at 180 °C. Quinoline and



2-methylquinoline were transformed to the respective THQ derivatives in yields of 95% and 93%, respectively. In 2022, Sun's group used *in situ*-generated Ir catalysts with chiral 2-pyridyl imidazoline ligands in an asymmetric TH of quinolines and other *N*-heteroaryl compounds. When a catalyst loading of 0.2 mol% with 2.5 equiv FA was utilized in water at RT, the hydrogenation of 2-methylquinoline resulted in 92% yield with 62% ee in 6 h.<sup>88</sup> Maji and Choudhury,<sup>89</sup> achieved the TH of quinolines with a Cp\*Ir half-sandwich complex bearing an uracil-based bifunctional abnormal *N*-heterocyclic carbene (NHC) ligand soluble in water. Employing a catalyst loading of 0.06 mol% and the hydrogen source as HCOOH/HCOONa buffer solution, they achieved 99% product yield (45 °C, 1 h). Cabrero-Antonino *et al.*<sup>90</sup> reported the first homogeneous earth-abundant metal catalyst for the TH of quinolines in 2017. The active species was generated *in situ* by combining (CoBF<sub>4</sub>)<sub>2</sub>·6H<sub>2</sub>O with tris(2-((diphenylphosphino)phenyl) phosphine ligand to hydrogenate quinolines, giving up to 99% conversion. Similar results were obtained with the analogous well-defined complex of Co under the same reaction conditions.

#### 4.1.1.3.3. Using ammonia borane as a hydrogen source.

Vermaak *et al.*<sup>91</sup> developed the first Ni(II)-catalyzed TH of quinolines, where ammonia borane (AB) was utilized as the source of hydrogen. They discovered that the precatalysts, an *in situ*-generated Ni(II)-bis(pyrazolyl)pyridine complex, effectively hydrogenated quinoline derivatives, achieving yields as high as 90% after 30 min at 25 °C. NMR analysis indicated that the presence of a hydride Ni(II) complex accounts for the TH of quinoline to 1,2,3,4-THQ, proceeding through the 1,4-dihydroquinoline intermediate. Jia *et al.*<sup>92</sup> described the efficient TH of quinolines to form 1,2,3,4-THQ with complexes based on Pd(II) containing NHC and bridged phenylene bis(thione) ligands, where AB was employed as the source of hydrogen under gentle reaction conditions. Notably, higher activities were observed with binuclear Pd(NHC) complexes relative to the Pd(NHC) mononuclear complexes under identical reaction conditions. Wu's group also reported TH of indoles and quinolines catalyzed by zirconium hydride, with AB being the source of hydrogen.<sup>93</sup> The yields of the hydrogenated products reached up to 94%, with good tolerance toward diverse functionalities. Preliminary mechanistic investigations suggest a concerted activation pathway involving both N-H and B-H bonds.<sup>93</sup>

Maji *et al.*<sup>94</sup> reported the hemilabile Mn complex with amine, benzimidazole, and sulfur-containing ligands for the TH of various quinoline derivatives, sourcing hydrogen from AB. The well-defined complex could hydrogenate quinolines to the corresponding THQ in up to 85% yield at 35 °C in THF. Bhatt and Natte<sup>95</sup> developed a no-ligand TH of various heteroarenes employing a commercial homogeneous RuCl<sub>3</sub>·xH<sub>2</sub>O precatalyst with AB as a hydrogen source. This method is simple, user-friendly, and accommodates a diverse range of functionalities, enabling even challenging heterocycle substrates to be reduced. Under optimal reaction conditions of 120 °C, 5–10 mol% catalyst loading, and 24 h

reaction time, quinoline and 2-methylquinoline were hydrogenated to their THQ derivatives in isopropanol in yields of 91% and 87%, respectively. Mao *et al.*<sup>96</sup> demonstrated Mn-catalyzed asymmetric TH of quinolines using AB hydrogen source in aqueous media. They reported the reduction of an array of quinoline substituted at position 2, to their THQ derivatives, yielding up to 97% and ee's as high as 99%. Furthermore, Chu *et al.*<sup>97</sup> also demonstrated the catalytic TH of quinolines to 1,2,3,4-THQs using Mn(I) PNP pincer complex **26** (Fig. 7) with AB in the presence of KO<sup>t</sup>Bu.

4.1.1.3.4. Other hydrogenating agents. Fujita *et al.*<sup>98</sup> in 2004 developed an efficient approach to the TH of quinolines using a Cp\*Ir complex as the catalyst. This approach enabled the chemo- and regioselective TH of quinolines with isopropanol serving as the source of hydrogen, yielding a range of 1,2,3,4-THQs. They discovered that adding perchloric or triflic acid or other Brønsted acids was necessary to achieve protonation and activate the substrate for effective hydrogenation (Scheme 7). In 2017, He *et al.*<sup>99</sup> developed a highly efficient TH of quinolines employing Hantzsch ester as the hydrogen transfer agent using mild reaction conditions. Utilizing 2.5 equiv Hantzsch ester and 1 mol% load of Fe(OTf)<sub>2</sub> at 40 °C, quinoline was converted to THQ in 96% yield. Various methyl-substituted quinolines were also dehydrogenated with yields ranging 86–96%. Recently, methyl formate was employed as a hydrogen source in the TH of quinoline derivatives with an Ir(III) complex. Using 0.2 mol% catalyst loading and 10 equiv. methyl formate, quinoline was converted to THQ in 92% yield.<sup>100</sup> Gong *et al.*<sup>101</sup> also reported the Mn-catalyzed TH of quinolines and other *N*-heteroarenes. The molecular Mn complex catalyst system they developed employed 2-propanol or ethanol as the hydrogen source. This straightforward transformation demonstrates an efficient catalyst system and high tolerance for various functional groups. Overall, this advancement presents an effective and practical synthetic approach for producing useful heterocycles. Employing DFT studies revealed an outer-sphere mechanism, where the 3,4-dihydroquinoline pathway is preferred to either the 1,2- or 1,4-dihydroquinoline routes in the TH of quinoline to THQ. Additionally, the rate-limiting step involves transporting a hydride to the Mn center from propan-2-olate, which regenerates the catalyst.<sup>101</sup>

#### 4.1.1.3.5. Mechanistic considerations of TH reactions.

Maji *et al.*<sup>94</sup> proposed the mechanism illustrated in Scheme 8 for the Mn-catalyzed TH of quinolines with AB as the hydrogen donor. Initially, the reaction of Mn complex with

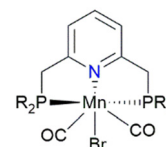
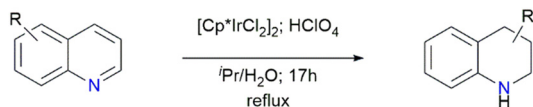


Fig. 7 Structure of Mn(I) PNP pincer complex **26**, R = <sup>t</sup>Bu.



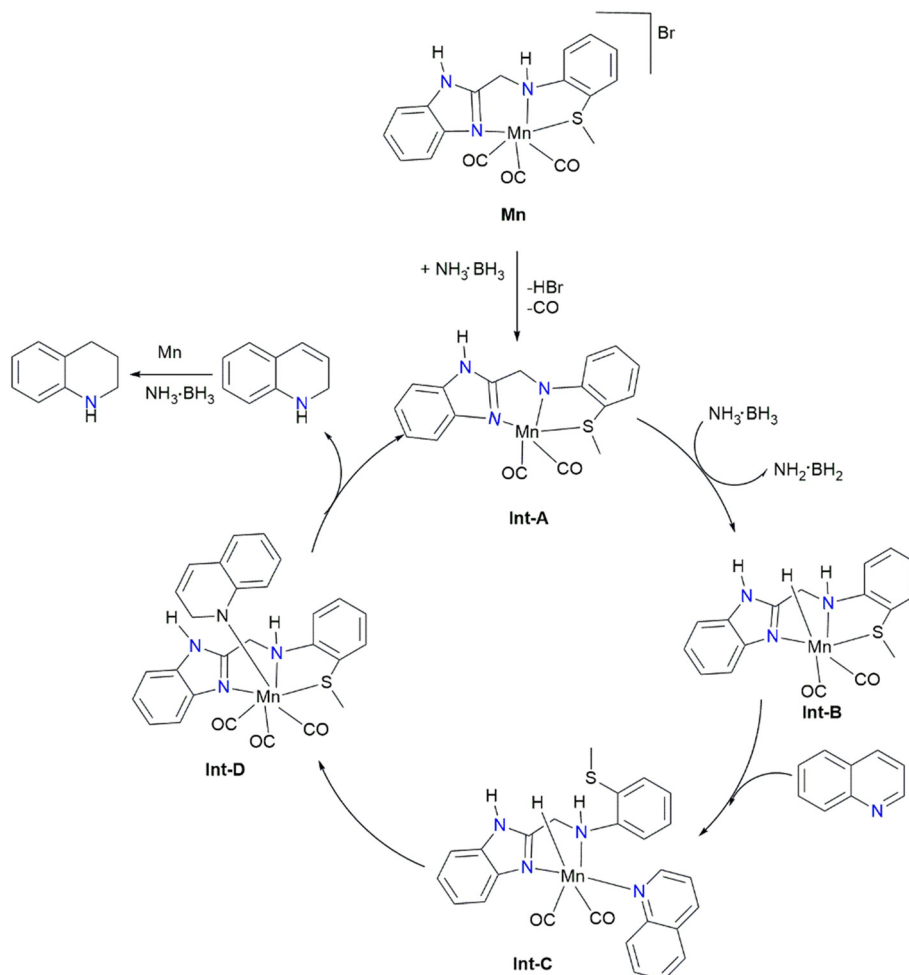


**Scheme 7** TH of quinolines with isopropanol as the hydrogen source.<sup>98</sup>

AB afforded the pentacoordinate intermediate (**Int-A**) when HBr and CO are eliminated *via* dehydrohalogenation promoted by AB.<sup>57,58</sup> Next, **Int-B** (Mn(I) hydride) was produced *via* dehydrogenating AB by **Int-A**, releasing H<sub>2</sub>N·BH<sub>2</sub>. Subsequently, the thiomethoxy side arm of the ligand is dissociated, and quinoline is bonded to the metal center, resulting in **Int-C**. Interestingly, adding an external source of ligand dramatically decreased the yield of 1,2,3,4-THQ, and the Mn(I) complex with a lightly bound hemilabile sulfur side arm displayed better activity relative to the other complexes with strongly bound ligands. Thereafter, the quinoline's C–N bond is incorporated into the Mn–H bond, affording an intermediate (**Int-D**). Afterwards, 1,2-dihydroquinoline is produced through proton migration from the N–H ligand backbone, regenerating **Int-A**, the active catalyst.

**4.1.1.4. Regioselective hydrogenation of carbocycles in quinolines.** In compounds with several aromatic components, the ring with the minimal resonance energy preferentially undergoes hydrogenation. For instance, it is well established that the hydrogenation of quinolines and related compounds occurs at the heteroaromatic ring, being the least aromatic.<sup>102</sup> However, Borowski *et al.*<sup>103</sup> hydrogenated certain polynuclear *N*-heteroaromatic compounds with bis(dihydrogen) Ru complex [RuH<sub>2</sub>(PCy<sub>3</sub>)<sub>2</sub>(H<sub>2</sub>)<sub>2</sub>], **27** (Fig. 8), and found the conversion of isoquinoline and quinoline to their corresponding 5,6,7,8-tetrahydro carbocycle-hydrogenated products under gentle conditions (Scheme 9). Their findings indicated that RuH<sub>2</sub>(PCy<sub>3</sub>)<sub>2</sub> complexes engage in η<sup>4</sup>-coordination with the carbocycle, leading to regioselective reduction under mild conditions.

Later, Urban *et al.*<sup>104</sup> in 2011 reportedly employed a chiral Ru complex with NHC ligands (**28**) in quinoxaline asymmetric hydrogenation, affording the corresponding carbocycle-hydrogenated products with good enantioselectivity. Notably, the NHC ligand greatly influences the regioselectivity, highlighting the impact of electronic tuning in catalyst design. Kuwano *et al.*<sup>105</sup> also researched



**Scheme 8** Mechanism for the TH of quinoline using AB as hydrogen source.<sup>94</sup>



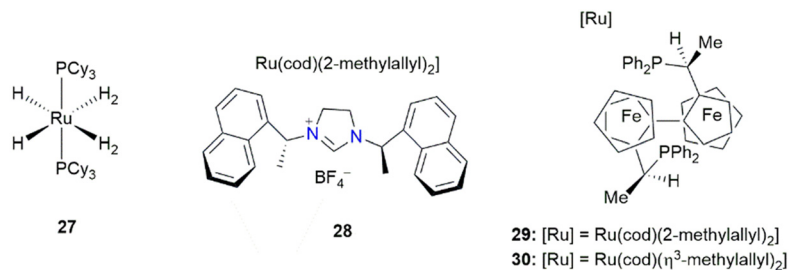


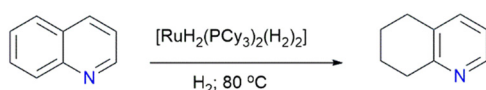
Fig. 8 Examples of Ru catalysts for the regioselective hydrogenation of carbocycles in quinolines.

the hydrogenation of isoquinolines and quinolines utilizing the Ru/PhTRAP (29) in asymmetric catalysis. Again, hydrogenating the carbocycle was preferred to the heterocycle in isoquinolines and quinolines. In a different analysis by Kuwano and colleagues, where the selective hydrogenation of isoquinoline carbocycles was accomplished using Ru(η-methylallyl)<sub>2</sub>(COD) together with the *trans*-chelate chiral PhTRAP (30) ligand, it was suggested that the diphosphine ligand's huge bite angle could be essential for the remarkable chemoselectivity.<sup>106</sup> Scheme 10 illustrates the plausible pathways suggested for the hydrogenation of quinoline carbocycles using Ru-based catalysts.<sup>105,106</sup>

Recently, Luo *et al.*<sup>107</sup> reported a highly selective homogeneous Ru-catalyzed hydrogenation of the carbocyclic ring in fused heteroarenes such as quinolines, isoquinolines, and quinoxalines. The catalyst system consists of a Ru complex with a chiral spiroketal-based diphosphine (SKP) ligand 31. The method gives excellent chemoselectivity, favoring 5,6,7,8-tetrahydro products over the conventional 1,2,3,4-tetrahydro counterparts. They also investigated various ligands in Ru-catalyzed quinoline hydrogenation using similar conditions as the SKP system.

The ligands (32–36 and 38, Fig. 9) gave inferior reactivity and selectivity, while 37 and 39 resulted in poor conversion. On the contrary, 40, an N-heterocyclic carbene, was highly reactive but lacked selectivity. Interestingly, the 2,2'-bipyridine ligand 41 favored the heterocycle-reduced product, indicating that the competing carbo/heterocycle hydrogenation pathways are influenced by ligand electronics and steric effects. Using [Ru(*p*-cymene)Cl<sub>2</sub>]<sub>2</sub> instead of Ru(methylallyl)<sub>2</sub>(COD) with 31 gave almost identical results, suggesting a common active Ru species in both cases. The mechanism involves an inner-sphere hydrogen transfer pathway, where an initial η<sup>4</sup>-coordination of the carbocycle to Ru facilitates metal-to-ligand hydride transfer, followed by sequential oxidative addition of H<sub>2</sub> and reductive elimination of C–H.

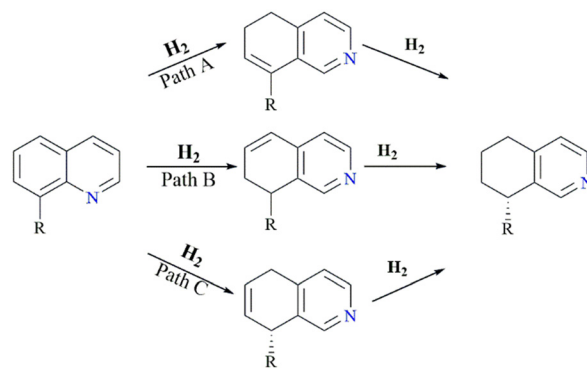
4.1.1.5. Full hydrogenation of quinoline to decahydroquinoline. Homogeneously catalyzed hydrogenation



Scheme 9 Carbocyclic regioselective reduction of quinolines.

of quinoline typically produces the THQ derivatives, whereas the decahydroquinoline (DHQ) derivatives require more stringent reaction conditions with heterogeneous catalyst systems.<sup>20</sup> In 2020, Chatterjee *et al.*<sup>59</sup> reported a one-pot dual catalysis for hydrogenating arenes and heteroarenes using the Ru complex [(η<sup>6</sup>-*p*-cymene)RuCl]<sub>2</sub>(μ-H–μ-Cl). They demonstrated that adding mercury or phenanthroline had little or no impact on reducing quinoline to THQ. Indications were that a molecular complex facilitates this transformation. On the contrary, fully hydrogenating THQ or quinoline was effectively halted when these poisons were present, implying that Ru nanoparticles account for the carbocyclic ring reduction. Considering their findings, they proposed that the full reduction of quinoline is achieved *via* “dual catalysis”, where an organometallic complex aids in the heterocycle hydrogenation, and NPs produced *in situ* facilitate the homocycle conversion.

Viereck *et al.*<sup>65</sup> recently introduced an innovative catalyst system for the diastereoselective and enantioselective complete reduction of naphthalenes and quinolines. Utilizing the earth-abundant Mo as a more sustainable transition metal, they strategically identified an oxazoline imino(pyridine) ligand framework. Using a large *tert*-butyl substituent on the pyridine ring proved essential for achieving high enantioselectivity, even though it is positioned further from the metal center. This extra steric hindrance likely prevents hydrogenation of the pyridine, thereby avoiding catalyst degradation and minimizing racemic background reactions that could lower the enantiomeric



Scheme 10 Suggested routes for hydrogenating isoquinoline carbocycles.<sup>105,106</sup>



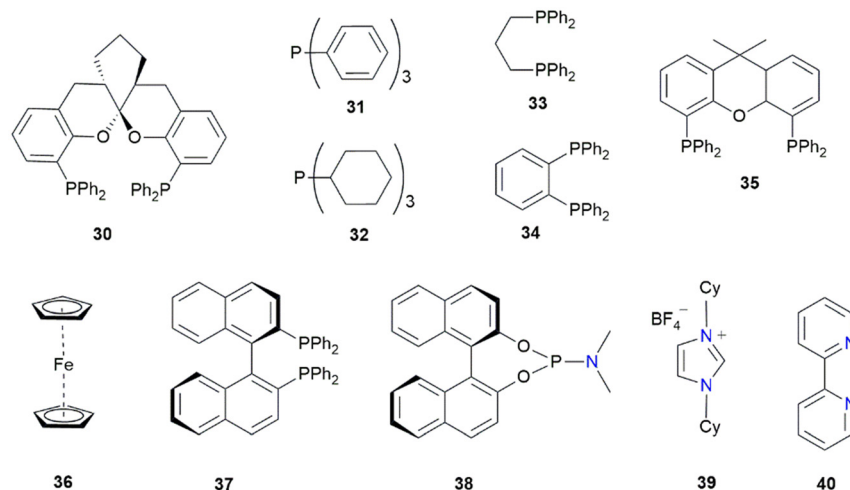


Fig. 9 Scope of ligands screened for the Ru-catalyzed hydrogenation of the carbocyclic ring in quinoline using the Ru(methylallyl)<sub>2</sub>(COD) precursor.

excess. A series of quinolines with 2,6-disubstitution is exposed to standard hydrogenation conditions. Remarkably, every 2,6-disubstituted quinoline was converted to a DHQ single diastereomeric product, establishing four stereocenters in one process.

Hydrogenating 2,6-dimethylquinoline gave a 40% yield with DHQ having over 98% ee. Furthermore, the hydrogenation of 2-methylquinoline led to a 17% yield, with its DHQ counterpart having 91% ee. As the position 6's substituent surged in size, specifically in 6-isopropyl-2-methylquinoline, the DHQ was obtained in 8% yield with a 77% ee. Altering the substituent at position 2 to a phenyl group substantially slowed the reaction, resulting in a mix of phenyl, heterocycle, and carbocycle reduction products, likely resulting from the greater steric hindrance. The varied product mix underscores the Mo catalyst's distinctive reactivity, as it facilitates arene ring hydrogenation while promoting enantioselective heterocycle hydrogenation. The full reduction of the two rings in quinoline was peculiar to the 2,6-substitution and moving away to different substitution sites resulted in mixed products. Changing the heteroarene substitution hindered full reduction yielding a mixture with 18% carbocycle-reduced and 81% heterocycle-reduced products (98% ee). This suggests that the full hydrogenation of quinolines depends on their steric environment. Furthermore, quinolines without substitution next to a heteroatom did not get fully hydrogenated to DHQ; instead, a mix of heterocycle and carbocycle-reduced derivatives was detected.

#### 4.1.2. Reversible quinoline hydrogenation catalyst systems.

The quinoline/DHQ pair has shown promise as an LOHC system. However, research on the complete reduction of quinoline and the corresponding dehydrogenation of DHQ remains limited. Most studies have instead concentrated on the quinoline/THQ pair, which has a lower HSC of 2.3 wt%.<sup>108</sup> In 2009, Yamaguchi *et al.*<sup>109</sup> reported the first homogeneous catalyst system capable of effective and

reversible hydrogenation of quinolines with the same catalyst. The 5-trifluoromethylpyridonate Cp\*Ir complex **42** (Fig. 10) allowed nearly quantitative dehydrogenation of 2-methyl-1,2,3,4-THQ to 2-methylquinoline under reflux in *p*-xylene (20 h). The reaction was performed with 2 mol% **42** and repeated five times, with minimal efficiency loss. For hydrogenation, similar conditions were used, but in an H<sub>2</sub> atmosphere. At 110 °C and 1 bar H<sub>2</sub>, quinoline and 2-methylquinoline were converted to their hydrogenated counterparts in almost quantitative yield, and the reaction

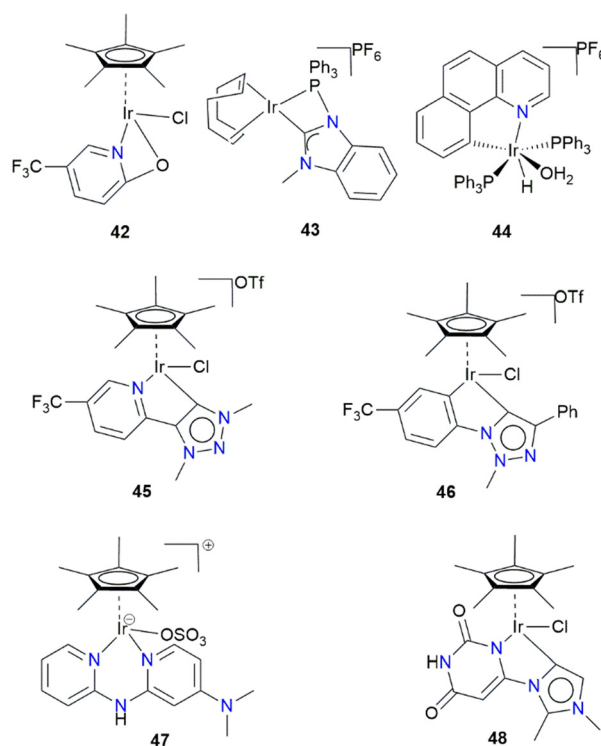


Fig. 10 Examples of Ir complexes used for dehydrogenating THQ.



time decreased significantly upon increasing the H<sub>2</sub> pressure to about 3 bar at 80 °C or 10 bar at 110 °C. The system allowed for reversible transformations between quinolines, repeated five times without a considerable drop in performance. The mechanism was reported later in 2011.<sup>110,111</sup>

Manas *et al.*<sup>112</sup> in 2015 reported on two Ir catalysts **43** and **44** for the reversible hydrogenation of quinaldine. Although neither system surpassed **42** in terms of dehydrogenation efficiency, both **43** and **44** are much more efficient for the hydrogenation of quinaldine. Vivancos *et al.*<sup>113</sup> developed an effective approach for reversibly (de)hydrogenating derivatives of quinoline with a triazolylidene-based Ir complex, operating in water without additives under mild conditions. Complexes **45** and **46** were effective catalysts in both reactions, with the reaction greatly influenced by the partial pressure of hydrogen in the medium. Impressively, when using 0.5 mol% **47** at 90 °C, the hydrogenation of quinoline in water resulted in 100% conversion. Meanwhile, the reverse dehydrogenation at 100 °C with 2 mol% catalyst achieved 90% conversion.

These reversible catalytic transformations are highly efficient in aqueous media, with the shift between hydrogenation and dehydrogenation governed solely by the presence or absence of hydrogen gas.

Similarly, Wang *et al.*<sup>114</sup> in 2019 successfully performed both hydrogenation and dehydrogenation of the quinoline/THQ pair using the electron-rich Ir catalyst **48** in aqueous solution under mild conditions. However, the catalyst was not recycled in multiple hydrogenation–dehydrogenation cycles.

Choudhury's group successfully developed reusable, bifunctional Ir-based catalysts for (de)hydrogenation of *N*-heteroarenes in aqueous solution.<sup>115,116</sup> These catalysts, when used in aqueous media, were effective for (de)hydrogenation reactions. The key design features included the incorporation of an abnormal/normal *N*-heterocyclic carbene (*a/n*NHC)–Ir(III) to enhance the stability and robustness of the complex while facilitating efficient hydride transfer due to the strong sigma-donor properties of the *a/n*NHC ligand. In addition, a bifunctional metal–ligand unit to promote cleavage of H–H (or N–H) bonds through cooperative mechanisms was employed, and the incorporation of uracil nucleobase in the ligand structure provided solubility in water through hydrogen bonding in the complex's second coordination sphere. This design led to the development of Ir catalyst **48** with long-term durability; furthermore, it was capable of operating under mild conditions, and high product yields could be achieved. Ru complexes bearing multimodal proton-responsive CNN(H) pincer ligands were also found to demonstrate considerable activity in both quinoline dehydrogenation and hydrogenation.<sup>117</sup> Besides the platinum group metals (PGMs), a few earth-abundant metal complexes have been employed for the reversible hydrogenation of quinolines. In 2014, Chakraborty *et al.*<sup>118</sup> used a molecular Fe complex bearing a

pincer bis(phosphino) amine ligand for the hydrogenation and acceptorless dehydrogenation of *N*-heterocycles. Iron is appealing, owing to its low toxicity, cost, abundance, and having similar properties to Ir catalysts. The full conversion of 1,2,3,4-tetrahydroquinaldine requires a reaction in xylene at 140 °C for 30 h, using a catalyst loading of 3 mol%, whereas the reverse hydrogenation involves a reaction for 24 h in THF at 80 °C, at high pressure (5–10 bar H<sub>2</sub>), using 10 mol% of KO<sup>t</sup>Bu. Furthermore, the acceptorless, reversible hydrogenation reactions involving quinolines have been reported to proceed with a molecular Co complex and pincer aminobis(phosphine) [PN(H)P] ligand.<sup>119</sup> Dahiya *et al.*<sup>120</sup> reported a stable molecular Cp\*Co(III)-catalyst for the TH of quinoline derivatives and cyclic amines oxidative dehydrogenation in aqueous media. They reported that the hydrogenation is facilitated by FA as a hydrogen donor, whereas the dehydrogenation utilizes O<sub>2</sub> gas as the oxidant. These methods open new opportunities to explore air-stable Co catalysts for eco-friendly (de)hydrogenation processes.

**4.1.3. Dehydrogenation of tetrahydroquinolines.** In 2013, Wu *et al.*<sup>121</sup> reported an oxidant-free, flexible catalyst system for the acceptorless catalytic dehydrogenation of diverse *N*-heterocycles. They performed catalytic dehydrogenation of various 1,2,3,4-THQs under reflux (20 h) using 2,2,2-trifluoroethanol as solvent and 0.1 mol% of Ir complex **49** (Fig. 11) and obtained the corresponding quinolines in very high yields (up to 97%). Yao *et al.*<sup>122</sup> demonstrated the use of the pincer Ir complex (**50**) in transfer dehydrogenation of heterocycles and alkanes. For the hydrogen source, *tert*-butylethylene was employed, and upon activation with NaO<sup>t</sup>Bu at 120 °C in *p*-xylene, 1,2,3,4-THQ was dehydrogenated to quinoline (76% yield). The transfer dehydrogenation of *N*-heterocycles was satisfactorily achieved, despite the substrates requiring a large loading of ~1–5 mol% of the Ir catalyst. In 2019, Jeong *et al.*<sup>123</sup> examined the effect of substituents in a cyclopentadienyl ligand on the acceptorless dehydrogenation of 2-methyl-

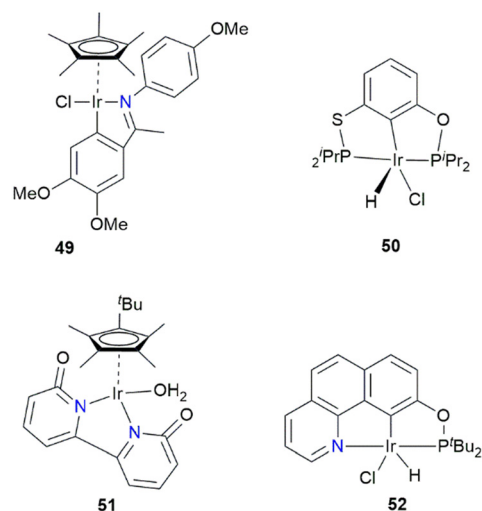


Fig. 11 Examples of Ir complexes used dehydrogenating THQ.



1,2,3,4-THQ catalyzed by Ir. The reactions proceeded in toluene at reflux for 20 h. The best-performing catalyst bearing bulky *tert*-butyl substituents exhibited excellent activity, affording the dehydrogenated product 2-methylquinoline. The activity of a series of Ir complexes, including **51**, with diverse substituents on the cyclopentadienyl follows the order  $t\text{Bu} > \text{Me} > \text{Et} > i\text{Pr} > \text{H}$ .<sup>123</sup>

NCP-type pincer Ir complex (**52**) bearing a robust benzoquinoline framework demonstrated efficient quinoline dehydrogenation. Quantitative product yields were obtained when THQ and tetrahydroisoquinoline were dehydrogenated at 150 °C with a catalyst load of 1 mol%.<sup>124</sup>

Muthaiah and Hong<sup>125</sup> reported the Ru-catalyzed dehydrogenation of various THQ derivatives with commercially available Ru–H complexes. Using 2.5 mol% catalyst loading, Shvo's catalyst quantitatively dehydrogenated tetrahydroisoquinoline at 165 °C in mesitylene (24 h). The 1,10-phenanthroline-5,6-dione Ru complex with Co(salophen) cocatalyst system was utilized in dehydrogenating several THQs. The system exhibited efficient activities, with various substrates, when 2.5 mol%  $[\text{Ru}(\text{phd})_3]_2^+$  catalyst and 5 mol% Co(salophen) cocatalyst loadings were used under ambient conditions.<sup>126</sup> Their initial studies compared the previously optimized phd/ZnI<sub>2</sub> catalyst with simple octahedral  $[\text{Fe}(\text{phd})_3]_2^+$  and  $[\text{Ru}(\text{phd})_3]_2^+$  complexes for THQ dehydrogenation. The phd/ZnI<sub>2</sub> system exhibited low activity, and the activity was lost after ~6–7 h, resulting in ≤20% conversion. The  $[\text{Fe}(\text{phd})_3]_2^+$  had a comparable rate on the onset but improved stability, while  $[\text{Ru}(\text{phd})_3]_2^+$  exhibited significantly higher activity with 93% quinoline yield achieved within 24 h. Adding Bu<sub>4</sub>NI (1 mol%) confirmed that the redox couple ( $\text{I}^-/\text{I}^{3+}$ ) facilitates aerobic oxidation of the hydrogenated catalyst. Noteworthy is that THQ was dehydrogenated under optimized conditions to afford 89% isolated product yield.<sup>126</sup> Wang *et al.*<sup>127</sup> dehydrogenated THQ derivatives utilizing pyrazolyl-indolylpyridine Ru(II) organometallics in good yields (up to 93%). With a monohydrido-bridged dinuclear Ru catalyst in the acceptorless dehydrogenation of heterocycles, THQ was converted to quinoline in 85% yield with 1 mol% catalyst loading at 135 °C in toluene.<sup>128</sup>

Homogeneous Pd catalysts have also been utilized in the dehydrogenation of THQs. For example, Wang *et al.*<sup>129</sup>

achieved 92% yield when THQ was dehydrogenated using Pd(MeCN)<sub>2</sub>Cl<sub>2</sub> in dichloroethane at 120 °C in the presence of O<sub>2</sub>. Similarly, when using 5 mol% Pd(OAc)<sub>2</sub> with a neocuproine catalyst system in DMF, THQ afforded quinoline in 83% isolated yield in 1 h.<sup>130</sup> An inexpensive CuI catalyst was used by Jung and coworkers<sup>131</sup> for the dehydrogenation of 1,2,3,4-THQ at RT under mild conditions. Notably, using 10 mol% each of CuI and di-*tert*-butyl azodiformate and 20 mol% 4-dimethylaminopyridine additives enhanced the dehydrogenation to afford up to 92% quinoline yield.<sup>131</sup> Shen *et al.*<sup>132</sup> used 2 mol% Cu(I) complex **53** (Fig. 12) to dehydrogenate THQs in utilizing 1,2-dichlorobenzene and O<sub>2</sub> (120 °C, 3 h) to afford a high yield. This method is advantageous as it is carried out in the absence of additives. Zumbrägel *et al.*<sup>133</sup> used oxovanadium(V) complex with gentle reaction conditions under O<sub>2</sub> to dehydrogenate THQs.

When using 10 mol% of the complex in water (60 °C, 1 bar O<sub>2</sub>, 48 h), 91% quinaldine was obtained from tetrahydroquinaldine. In 2020, Bera *et al.*<sup>134</sup> reported dehydrogenating N-heterocycles using a Ni catalyst and molecular oxygen. Impressively, the system converted THQ to quinoline in excellent yield.

## 4.2. Carbazoles

Carbazole is an alternative LOHC with a high HSC (6.7 wt%) and stability under favourable conditions, hence ideal for prolonged storage. Nonetheless, with a 68–70 °C melting point, it becomes solid at RT following oxidation.<sup>135</sup> The structures of selected carbazoles used as LOHCs are illustrated in Fig. 13.

Wang *et al.*<sup>6</sup> studied dehydrogenating *N*-ethylperhydrocarbazole using Ir pincer complexes **54–56** (Fig. 14). They tested the three catalysts at 200 °C and found that they produced varied, partially dehydrogenated products: *N*-ethyloctahydrocarbazole, *N*-ethyltetrahydrocarbazole, and *N*-ethylcarbazole (NEC). Catalyst **56** showed the highest activity, where NEC was converted within 9 h to yield 70% *N*-ethyloctahydrocarbazole and 30% *N*-ethyltetrahydrocarbazole. Extending the reaction time led to further dehydrogenation, resulting in 82% *N*-ethyltetrahydrocarbazole and 18% NEC, with a TON that reached 436. Lowering the temperature to 150 °C, the efficiency dropped significantly, producing only 23% *N*-ethyloctahydrocarbazole and 2% *N*-ethyltetrahydrocarbazole.<sup>7</sup> No evidence of dehydrogenation was observed in experiments performed at 100 °C. This likely indicates that the high enthalpy of the substrate imposes thermodynamic limitations at lower temperatures.<sup>7</sup> According to later reports, the selective

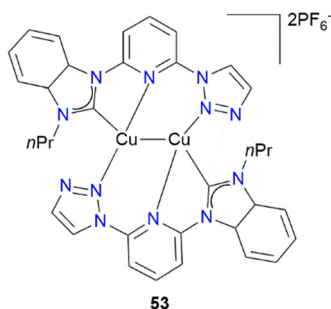


Fig. 12 Structure of Cu(I) complex for indoline dehydrogenation.

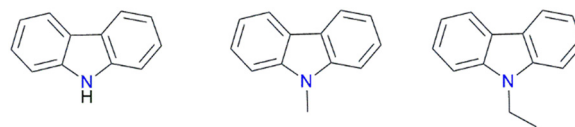


Fig. 13 Structures of selected carbazole derivatives used as LOHCs.



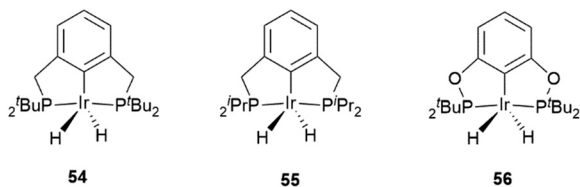


Fig. 14 PCP Ir pincer complexes used in dehydrogenating carbazoles.



Fig. 15 Structures of indole derivatives.

dehydrogenations of perhydroindoles and perhydrocarbazoles specifically occur at the five-membered rings.<sup>136</sup>

### 4.3. Indoles

Indoles (Fig. 15), structurally akin to carbazoles, have attracted interest as potential LOHC systems. These compounds are readily accessible and exhibit favorable LOHC characteristics, including positive kinetic and thermodynamic profiles for hydrogen release from perhydroindoles using relatively mild temperatures.<sup>137,138</sup> Table 5 details the properties of some commonly studied indole derivatives as LOHCs.

The (de)hydrogenation of indoles and their derivatives, such as 1-methylindole (1-MID), 2-methylindole (2-MID), *N*-ethylindole (NEID), and 7-ethylindole (7-EID), among others, has been primarily explored using heterogeneous catalyst systems.<sup>20,139</sup> For example, Li *et al.*<sup>140</sup> demonstrated the hydrogenation of 2-MID using a catalyst composed of 5 wt% Ru/Al<sub>2</sub>O<sub>3</sub> at temperatures between 120 and 170 °C, with a rapid conversion rate. The subsequent dehydrogenation of its hydrogenated form, 8*H*-2-methylindole, was achieved with a 5 wt% Pd/Al<sub>2</sub>O<sub>3</sub> catalyst at temperatures ranging from 160 to 200 °C, resulting in complete dehydrogenation within 4 h at 190 °C, without any side reactions. Compared to heterogeneous catalysts, the use of homogeneous catalysts in these transformations for applications in LOHCs is rather limited. The

homogeneously catalyzed (de)hydrogenation of indole derivatives is discussed in the sections that follow.

#### 4.3.1. Homogeneously catalyzed hydrogenation of indoles.

Asymmetric hydrogenation of indoles is among the direct and atom-economical approaches for synthesizing chiral indolines, as it directly converts the starting material without requiring additional functionalization steps.<sup>141</sup> A highly effective process in the hydrogenation of various *N*-protected indoles was developed using Ru and Rh complexes.<sup>142–144</sup> Baeza and Pfaltz<sup>145</sup> further advanced the field by developing an Ir/*N*,*P*-catalyzed hydrogenation system that gave high enantioselectivity but suffered from low reactivity. Despite these advances, hydrogenating simple, unprotected indoles efficiently using asymmetric synthesis is a persistent hurdle for organic chemists.

Wang *et al.*<sup>141</sup> in 2010, reported the first example of a highly enantioselective hydrogenation of simple indoles using Pd(OCOFCF<sub>3</sub>)<sub>2</sub>/(*R*)-*H*8-BINAP (BINAP = 2,2'-bis(diphenylphosphino)-1,1'-binaphthyl, 57), activated using a Brønsted acid (Scheme 11). Notably, 2-methyl-1*H*-indole was readily hydrogenated. Up to 95% conversion and 91% ee were achieved when using 2.4 mol% (*R*)-*H*8-BINAP and 2 mol% Pd(OCOFCF<sub>3</sub>)<sub>2</sub> for 24 h at room temperature. The researchers proposed that the reaction's enantioselectivity results from the reversible protonation of the substrate, which allows selective hydrogenation of only the targeted enantiomer of the activated indole.

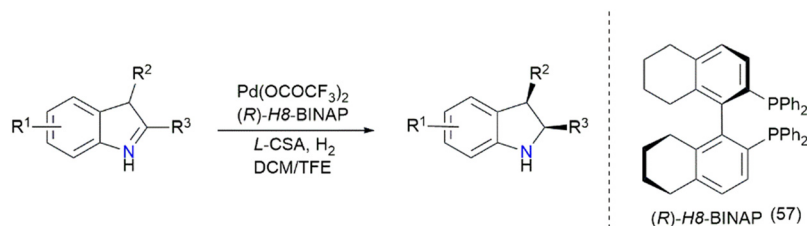
Núñez-Rico *et al.*<sup>146</sup> subsequently demonstrated the asymmetric hydrogenation of unprotected indoles employing *in situ*-generated Ir complexes obtained as a single enantiomer from phosphine–phosphite (P–OP) ligand 58 (Fig. 16). The hydrogenation of 2-methyl-1*H*-indole with 1 mol% Ir precatalyst in THF (rt, 80 bar H<sub>2</sub>), using stoichiometric quantities of sulfonic acid additives, resulted in 2-methylindoline. Interestingly, the conversion was dependent on the acid strength, where organic acids gave conversions of up to 20% while the stronger sulfonic acid derivatives elevated the conversions up to ~80%. Several reaction conditions were investigated, encompassing the reaction time, solvent type, and catalyst loading. Using the optimal reaction conditions, various indole derivatives were successfully hydrogenated to achieve high conversions (up to 92%) and 91% ee.<sup>146</sup>

Table 5 Properties of some commonly studied indole derivatives as LOHCs<sup>20,53,54</sup>

Indole/carbazole derivative	mp (°C)	bp (°C)	HSC (wt%)	Δ <i>H</i> (kJ mol <sup>-1</sup> H <sub>2</sub> )	Ref.
Indole/8 <i>H</i> -indole			6.4	53.6	20
1-MID/8 <i>H</i> -1-MID	–20/–25	239/230	5.76	51.9	20
2-MID/8 <i>H</i> -2-MID	57	273	5.76	51.7	20
NEID/8 <i>H</i> -NEID	–17.8	253.5	5.23		
7-EID/8 <i>H</i> -7-EID	–14/–20	230/230	5.23		
H-Carbazole	246.3		6.7	48.1	54
<i>N</i> -Methylcarbazole	89		6.2	49.1	54
<i>N</i> -Ethylcarbazole	70	363	5.7	47.8	53, 54

1-Methylindole (1-MID), 2-methylindole (2-MID), *N*-ethylindole (NEID), 7-ethylindole (7-EID), 8-ethylindole (8-EID).





**Scheme 11** Enantioselective reduction of unprotected indoles.<sup>141</sup>

Wen *et al.*<sup>147</sup> demonstrated that an effective catalyst system using a Rh/ZhaoPhos complex performs remarkably in acidic media. Various substituted indoles were reduced, resulting in appreciable enantioselectivities. Impressively, 2-methylindole was hydrogenated to afford 2-methylindoline in 98% yield and 98% ee with a substrate/[Rh(COD)Cl]<sub>2</sub>/ligand ratio = 100/0.50/1.0 (rt, 40.53 bar H<sub>2</sub>, 48 h).<sup>147</sup> In another study, the conversion of indole to indoline was accomplished in quantitative yield when using a catalytic system derived from [(η<sup>6</sup>-*p*-cymene)RuCl]<sub>2</sub>(μ-H-μ-Cl) (90 °C, 50 bar H<sub>2</sub>, 40 h). After combing various approaches comprising kinetic studies, *in situ* reaction monitoring, electron microscopy, and poisoning evaluations, the suggestion was made that the initial Ru complex functions as a precatalyst, and the heteroarene reductions are rather facilitated by a monomeric Ru complex.<sup>59</sup> Table 6 provides a summary of the catalysts for homogeneous hydrogenation of the various *N*-heterocyclic LOHCs discussed above.

**4.3.2. Dehydrogenation of indolines.** Complex 56 acts as an active catalyst for dehydrogenating perhydroindole, but only releases one equivalent of H<sub>2</sub> after heating at 200 °C for 3 h. Further heating for 3 days does not lead to additional dehydrogenation, which indicates that dehydrogenation proceeds only over the C–N bond, not the C–C bond. The catalytic dehydrogenation of *N*-methylperhydroindole, a tertiary amine, was explored in an effort to avoid the formation of imines. At 150 °C, 2.9 wt% H<sub>2</sub> was discharged after a week. Nearly complete dehydrogenation to the *N*-methyltetrahydroindole intermediate was realised, but dehydrogenation to *N*-methyl indole could not proceed further. Within an enclosed reactor charged with a hydrogen acceptor, about 92% *N*-methyltetrahydroindole and 7% *N*-methylindole were observed after 6 days at 150 °C. At 200 °C, the reaction mixture reached a 3:1 equilibrium between *N*-methyltetrahydroindole and *N*-methylindole, eliminating

over 4 wt% hydrogen. Thus, the kinetic barrier to dehydrogenation is overcome at higher temperatures, leading to thermodynamic control.<sup>148</sup>

Later, Brayton and Jensen,<sup>136</sup> explored the solvent-free dehydrogenation of various perhydroindolic substrates, including *N*-methylperhydroindole (MePHI), using Ir complex 56. The dehydrogenation of the heterocyclic ring in all indolic molecules commenced at 170 °C, while the cyclohexane ring remained unaffected until 200 °C. Consequently, the reactions were conducted at 195 °C to achieve an optimal dehydrogenation rate, without affecting the cyclohexane ring. To recover the products, filtration through an alumina plug or distillation was employed. MePHI gave a quantitative yield with 1 mol% of complex 56 after 48 h. However, benzoyl perhydroindole, perhydro-2-methylindole, perhydroindole, and perhydrooskatole exhibited low dehydrogenation yields of 6%, 1.5%, 3%, and 2.5%, respectively, with only slight improvements achieved when both catalyst loading and reaction time were increased.

Wang *et al.*<sup>114</sup> achieved a 97% conversion when indole was hydrogenated at 120 °C with an electron-rich Ir complex bearing a dipyrindyl amine ligand, using just 0.2 mol% catalyst loading. Additionally, the rare-earth praseodymium catalyst was developed to efficiently dehydrogenate indoline in high yield. Utilizing 7.5 mol% catalyst loading and 15 mol% 2,3-dichloro-5,6-dicyano-1,4-benzoquinone (DDQ) additive, indoline was dehydrogenated to 98% (1 bar O<sub>2</sub>, 12 h). This approach showed excellent compatibility with various functional groups, such as quinoline, under mild conditions (Scheme 12).<sup>149</sup>

In 2020, Kawauchi *et al.*<sup>150</sup> used Grubb's catalyst to perform the aerobic dehydrogenation of *N*-heterocycles. Using 0.1 mol% catalyst in EtOAc for 46 h, indoline was dehydrogenated in 90% yield at 70 °C.<sup>150</sup> Ru hydride complexes with a pyrazolyl-(2-indol-1-yl)-pyridine ligand effectively catalyzed the acceptorless dehydrogenation of *N*-heterocycles, showcasing high catalytic efficiency across a wide range of substrates. Notably, indoline was converted into 82% yield of indole. Substrates of indoline featuring a 2-Ph, 2-Me, or 3-Me groups were also dehydrogenated efficiently, resulting in indoles with yields ranging from 78% to 91%.<sup>127</sup> Osmium polyhydride was also identified as an efficient catalyst precursor for dehydrogenating cyclic amines to aromatic heterocycles. With 10 mol% catalyst loading and a temperature of 140 °C, excellent conversion of 2-methylindoline to 2-methylindole was achieved.<sup>151</sup> Liu's

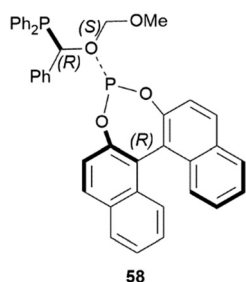


**Fig. 16** Structure of the P-OP ligand.



**Table 6** Summary of catalysts for homogeneous hydrogenation of N-heterocyclic LOHCs

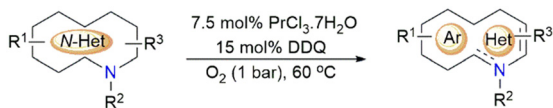
Catalyst	Substrate/product	Conv./yield(%)	Selectivity (%)	Ref.
Co-Tetrachlorophosphine	Quinoline/1,2,3,4-1,2,3,4-THQ	>99	—	76
[WCl(η <sup>5</sup> -Cp)(CO) <sub>3</sub> ]	Quinoline/1,2,3,4-THQ	94	—	77
[Ni(TIM(PAR) <sub>2</sub> ) <sub>3</sub> ](NTf <sub>2</sub> )	Quinoline/1,2,3,4-THQ	99	—	78
NNP-Mn(I)	Quinoline/1,2,3,4-THQ	>99	—	79
CN <sup>H</sup> C-Mn	Quinoline/1,2,3,4-THQ	97	—	80
Imidazolylidene-Mn(I)	Quinoline/1,2,3,4-THQ	20	—	81
AgOTf	2-Methylquinoline/1,2,3,4-THMQ	98	—	85
[Ir(cod)Cl] <sub>2</sub> /hydrosilanes	Quinoline/1,2,3,4-THQ	94	—	86
Ru(PPh <sub>3</sub> ) <sub>3</sub> Cl <sub>2</sub>	Quinoline/1,2,3,4-THQ	95	80	87
	2-Methylquinoline/1,2,3,4-THMQ	93	100	
Ir/imidazoline	2-Methylquinoline/1,2,3,4-THMQ	92	62 (ee)	88
Cp*Ir/uracil-NHC	Quinoline/1,2,3,4-THQ	99	—	89
(CoBF <sub>4</sub> ) <sub>2</sub> ·6H <sub>2</sub> O/phosphine	Quinoline/1,2,3,4-THQ	99	—	90
Ni(II)-bis(pyrazolyl)pyridine	Quinoline/1,2,3,4-THQ	97	—	91
NHC-Pd(II)-SCS	Quinoline/1,2,3,4-THQ	95	—	92
Cp <sub>2</sub> ZrH <sub>2</sub>	Quinoline/1,2,3,4-THQ	94	—	93
Mn-benzimidazole	Quinoline/1,2,3,4-THQ	85	—	94
RuCl <sub>3</sub> ·xH <sub>2</sub> O	Quinoline/1,2,3,4-THQ	91	—	95
	2-Methylquinoline/1,2,3,4-THMQ	87	—	
Mn(I) PNP	Quinoline/1,2,3,4-THQ	97	99 (ee)	96, 97
Cp*Ir	Quinoline/1,2,3,4-THQ	93	—	98
Fe(OTf) <sub>2</sub>	Quinoline/1,2,3,4-THQ	96	—	99
Ir(III) N <sup>^</sup> N	Quinoline/1,2,3,4-THQ	92	—	100
Mn-PNP	Quinoline/1,2,3,4-THQ	99	—	101
Mn(I) PNP	Quinoline/1,2,3,4-THQ	94	—	102
[RuH <sub>2</sub> (PCy <sub>3</sub> ) <sub>2</sub> (H <sub>2</sub> ) <sub>2</sub> ]	Quinoline/5,6,7,8-THQ	100	99	103
	Isoquinoline/5,6,7,8-THIQ	88.5	100	
Ru/PhTRAP	2-Phenylquinoline/5,6,7,8-THpQ	97	97	104
Ru-Ph-SKP	Quinoline/5,6,7,8-THQ	>99	>99	105
[{(η <sup>6</sup> -p-Cymene)RuCl] <sub>2</sub> (μ-H-μ-Cl)]	Quinoline/DHQ	>99	98 (ee)	65
Mo/oxazoline imino(pyridine)	2,6-Dimethylquinoline/2,6-dimethylDHQ	100	98 (ee)	64
	2-Methylquinoline/2-methylDHQ	100	91 (ee)	
Pd(OOCOCF <sub>3</sub> ) <sub>2</sub> /(R)-H8-BINAP	2-MID/2-Methylindoline	95	91 (ee)	141
Ir/P-OP	2-MID/2-Methylindoline	80	91 (ee)	146
Rh/ZhaoPhos	2-MID/2-Methylindoline	99	98 (ee)	147

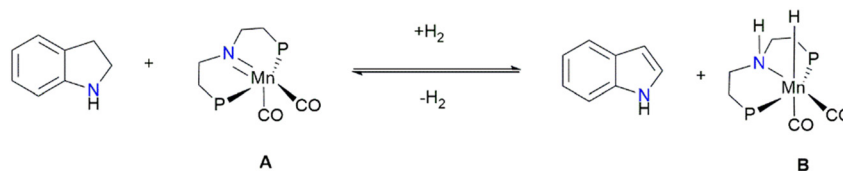
group also developed a technique involving 2 mol% of copper complex **46**, with 10 mol% of TEMPO additive and oxygen as an oxidant, at RT in THF, to afford high yields of indoles.<sup>132</sup>

**4.3.3. Reversible hydrogenation of indoles.** Chakraborty *et al.*<sup>118</sup> demonstrated the reversible N-heterocycles (de) hydrogenation using molecular Fe catalysts. Using 3 mol% catalyst loading and refluxing in xylene for 30 h, 2-methylindoline was dehydrogenated in 86% yield. Similarly, 2-MID was hydrogenated up to 69% yield in 24 h, using 3 mol% catalyst loading and 10 mol% of KO<sup>t</sup>Bu in THF at 80 °C. Interestingly, using a Co catalyst,<sup>119</sup> 2-methylindoline was quantitatively converted at 150 °C in xylene, whereas the reverse hydrogenation produced only 19% yield at 120 °C. Søgaard *et al.*<sup>139</sup> developed a biphasic catalytic system for hydrogen storage using the 2-MID/2-methylindoline pair,

where Crabtree's catalyst ([Ir(COD)(py)(PCy<sub>3</sub>)]PF<sub>6</sub>) was immobilized in [PPh<sub>4</sub>][NTf<sub>2</sub>] with PPh<sub>3</sub> as a stabilizing ligand. The system demonstrated efficient dehydrogenation at 130 °C and was recyclable with minimal loss in activity. However, complete hydrogenation was not achieved at 30 bar H<sub>2</sub> pressure. The dehydrogenation rate did show good Arrhenius behavior, exhibiting an apparent activation energy of 127.3 kJ mol<sup>-1</sup>. While the catalyst's activity decreased slightly during recycling, it remained effective for both dehydrogenation and hydrogenation. The hydrogenation rate was slower than the dehydrogenation rate, indicating the need for further optimization. Overall, this biphasic system offers the potential for reversible hydrogen storage and release at reduced temperatures.

Zubar *et al.*<sup>152</sup> reported an efficient method for the chemoselective hydrogenation and acceptorless dehydrogenation of N-heterocycles using a molecular Mn complex (Scheme 13). Indole was hydrogenated using 2 mol% of the Mn complex at 100 °C and 50 bar H<sub>2</sub> for 36 h and 5 mol% of the base, affording 92% indoline yield. This catalytic system is compatible with various functional groups, producing the reduced heterocycle derivatives with high yields. Further analysis indicated a mechanism involving

**Scheme 12** Aerobic dehydrogenation of N-heterocycles using rare-earth metal catalysts.<sup>147</sup>



**Scheme 13** Mechanism for the Mn-complex-mediated reversible hydrogenation of indole.<sup>152</sup>

metal–ligand cooperativity. Various substituted indoles were also analyzed under the established reaction conditions, resulting in the respective indoline derivatives in appreciable yields. The dehydrogenation of indoline under oxidant-free conditions using 1 mol% Mn complex (120 °C, 24 h) led to 89% indole. Notably, hydrogenation commences with the activation of the complex by KO<sup>t</sup>Bu, forming active species **A**, which then reacts with H<sub>2</sub> to generate H–N–Mn–H species **B**, facilitating indole conversion to indoline. In the dehydrogenation, species **A** converts indoline to indole, forming species **B**, which subsequently releases H<sub>2</sub>.

#### 4.4. Other potential LOHC candidates based on N-heterocycles

**4.4.1. Naphthyridines.** Naphthyridine (Fig. 17) has recently been proposed as a potential LOHC. Fujita *et al.*<sup>153</sup> studied the homogeneously catalyzed dehydrogenation of 2,6-dimethyldecahydro-1,5-naphthyridine and hydrogenation of 2,6-dimethyl-1,5-naphthyridine using Cp\*Ir catalysts (Fig. 18).

The naphthyridine structure, with two distanced nitrogen atoms, prevents bidentate coordination to the metal center. Using 5 mol% catalyst loading, Cp\*Ir complex (**59**) bearing a bipyridonate ligand selectively dehydrogenated 2,6-dimethyldecahydro-1,5-naphthyridine to 2,6-dimethyl-1,5-naphthyridine in quantitative yield at 138 °C in *p*-xylene. Similarly, the reverse hydrogenation reaction afforded a stereoisomeric mixture in 92% yield; however, the catalyst showed possible deactivation at 100 °C under H<sub>2</sub> (61 bar). Shifting to a Cp\*Ir complex (**60**) bearing a robust phenanthroline-2,9-dione ligand led to a nearly quantitative hydrogenation yield and a 98% dehydrogenation yield, confirming high catalytic activity. Successive hydrogenation and dehydrogenation reactions gave yields that reached 100% and 92%, respectively.

**4.4.2. Pyrazines.** Pyrazines (Fig. 19) have also emerged as promising candidates for LOHCs. In 2017, Fujita *et al.*<sup>154</sup> reported a novel technique for the reversible transformation between 2,5-dimethylpiperazine and 2,5-dimethylpyrazine using Ir-catalyzed (de)hydrogenation. Although its hydrogen gravimetric capacity is modest (5.3 wt%) compared to other

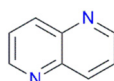


**Fig. 17** Structure of naphthyridine.

nitrogen-containing hydrogen storage systems, its solvent-free dehydrogenation is commendable.

2,5-Dimethylpiperazine was obtained quantitatively when using 0.50 mol% **61** (Fig. 20) and 1.0 mol% 6,6'-dihydroxy-2,2'-bipyridine, and a hydrogen/solvent (H/S) ratio of 60 (30 mmol hydrogen uptake in 0.50 mL solvent) was achieved.

Under optimal catalytic conditions, reversible hydrogenation was achieved in one vessel, in which the reaction was repeated four times without catalytic loss, as illustrated in Scheme 14. This system demonstrates an efficient hydrogen storage method with a high H/S ratio of 30 (30 mmol hydrogen in 1.0 mL solvent).

Solvent-free interconversion between **a** and **b** was also investigated with 78% hydrogenation efficiency recorded. Employing this approach resulted in the storage of 1144 mL (46.8 mmol) of hydrogen using 2.18 mL of 2,5-dimethylpyrazine.

## 5. Techno-economic considerations for aromatic and heteroaromatic LOHCs

The techno-economic viability of aromatic and heteroaromatic LOHC systems is governed by a set of interrelated descriptors that link molecular structure and catalytic performance to system-level feasibility. Key parameters include operating temperature and heat demand, hydrogen release kinetics, catalyst cost and lifetime, hydrogen purity, and long-term carrier stability. Together, these factors determine capital expenditure (CAPEX), operating costs (OPEX), and application suitability.

A dominant techno-economic constraint for both aromatic and heteroaromatic LOHCs is the high endothermicity of the dehydrogenation step, which typically requires operating temperatures in the range of 200–350 °C. Such elevated temperatures impose significant penalties in terms of heat management, reactor materials, start-up energy demand, and

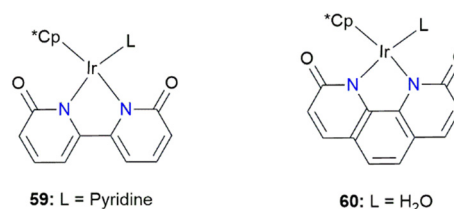


**Fig. 18** Structures of Ir complexes **59** and **60**.





Fig. 19 Structure of pyrazine.

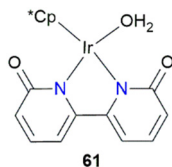
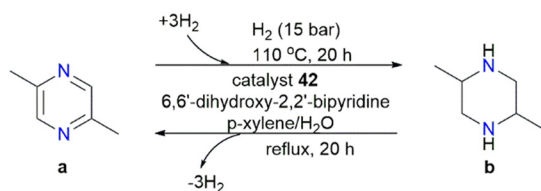


Fig. 20 Structure of Cp\*Ir complex 61.

Scheme 14 Method for interconverting compounds a and b through reversible hydrogenation catalyzed by 61.<sup>154</sup>

system integration, particularly for mobile or on-board applications. While heteroaromatic LOHCs may benefit from heteroatom-induced electronic effects that lower activation barriers and improve kinetics, these systems generally remain within a temperature regime best suited to stationary or hybrid energy storage concepts, where waste heat integration can partially offset the thermal demand.<sup>155–157</sup>

Beyond thermodynamics, hydrogen release kinetics directly influence reactor size and hydrogen throughput. Slow dehydrogenation rates necessitate larger reactors and longer residence times, increasing system footprint and capital cost. Aromatic LOHCs often exhibit sluggish kinetics in the absence of high temperatures or highly active catalysts, whereas heteroaromatic LOHCs can show enhanced rates due to polar functionalities or metal–ligand cooperative activation pathways. However, these kinetic advantages must be balanced against catalyst stability and selectivity under prolonged operation, underscoring the importance of catalyst robustness from a techno-economic perspective.<sup>156,158</sup>

Catalyst cost, lifetime, and recyclability represent another critical techno-economic descriptor, particularly for systems relying on homogeneous catalysis. Both aromatic and heteroaromatic LOHCs frequently employ precious-metal catalysts (*e.g.*, Ru, Ir, Pd), making high turnover numbers, long operational lifetimes, and efficient catalyst recovery essential for economic viability. Catalyst degradation or difficult separation can substantially increase operating costs and limit scalability.<sup>158,159</sup> In parallel, the purity of the released hydrogen plays a decisive role in downstream processing costs; even trace contaminants can necessitate

additional purification steps, particularly for fuel-cell applications.<sup>160</sup>

Finally, the availability, synthesis cost, and long-term chemical stability of the LOHC medium itself significantly impact system lifetime and operating expenditure. Carriers that exhibit high robustness over repeated hydrogenation–dehydrogenation cycles offer clear economic advantages, whereas degradation or side-product formation reduces effective hydrogen capacity and necessitates carrier replacement.<sup>155,157</sup> Overall, these considerations highlight that the techno-economic performance of aromatic and heteroaromatic LOHCs is dictated by trade-offs between hydrogen capacity, operating conditions, catalytic efficiency, and carrier durability, rather than by any single parameter in isolation.

## 6. Gaps in the literature

We have established that the following appear to be current gaps in the literature pertaining to the homogeneously catalyzed (de)hydrogenation of LOHCs (addressed further below).

- Limited literature on the dehydrogenation of homocyclic compounds using homogeneous catalysis (as far as we are aware, only one homogeneous catalytic system has been described for reversible hydrogen storage/release, and it utilizes an Ir pincer complex).
- A paucity of literature on homogeneous catalysts for the (de)hydrogenation of benzyltoluene (BT) and dibenzyltoluene (DBT).
- A paucity of literature on the complete/full hydrogenation of N-heterocyclic LOHCs.
- Apparently, no information is available on large-scale demonstrations with homogeneous systems.

In addressing the homogeneous (de)hydrogenation of potential homocyclic LOHCs, efforts to date have focused on the hydrogenation of toluene and benzene to produce the corresponding cyclohexane, with limited literature on other potential homocyclic LOHCs. Furthermore, to our knowledge, only one homogeneous catalyst system has been described for the reversible hydrogen storage employing an Ir pincer complex for homocyclic LOHCs. The paucity of studies on the (de)hydrogenation of homocyclic systems, such as DBT and BT, also represents a significant gap in the field. With their potential for high hydrogen storage capacities and stability, these systems warrant further investigation, particularly using homogeneous catalysts with tunable ligand environments. Furthermore, there is very little information on the complete/full (de)hydrogenation of critical heterocyclic LOHC candidates such as quinolines, indoles, and carbazoles. It appears that most of the catalytic systems reported to date for the (de)hydrogenation often result in partially (de)hydrogenated products. For instance, the quinoline/DHQ pair with HSC 7.2 is a promising LOHC candidate. However, research on hydrogenating quinoline completely and the corresponding dehydrogenation of DHQ



remains limited. Most studies have instead concentrated on the quinoline/THQ pair, which has a lower HSC of 2.3 wt%.

It is recommended that future research be focused on the development of efficient homogeneous catalyst systems for the complete (de)hydrogenation of LOHC pairs that have shown promise to date. Studies should also be directed at developing dual-functional catalysts capable of both hydrogenation and dehydrogenation with high efficiency.

## 7. The role of homogeneous catalysts in industrial processes

For many years, homogeneous catalysts have been important components of the chemical and material industries. It is impossible to overstate their importance in the efficient production of fine chemicals and materials with high levels of product selectivity, low temperature requirements, and other moderate reaction conditions. In addition to contributing to minimizing the costs to businesses, homogeneous catalysts can be fine-tuned to enhance their reactivity, selectivity, and robustness.<sup>161–165</sup> Homogeneous catalysts are relatively easily studied during their reactions because of their molecular nature. Unquestionably, these are the reasons why many of them are still used by industries decades after they first appeared.

For example, the Cativa process used to produce acetic acid efficiently *via* methanol carbonylation, using an Ir catalyst  $[\text{Ir}(\text{CO})_2\text{I}_2]$ , has been in use for almost three decades now after its development by BP Chemicals.<sup>166,167</sup> The Cativa process is an improved version of the Monsanto process, which makes use of Rh instead of Ir, and requires the presence of excess water and several drying columns for product drying.<sup>168</sup> Although the Cativa process is promoted by the presence of Ru as a cocatalyst, the formation of propanoic acid as a byproduct is reduced.<sup>166</sup>

It is considered relevant to include mention here of the synthesis of pharmaceuticals and other important complex molecules on commercial scales *via* the widely known Suzuki–Miyaura carbon–carbon bond cross-coupling reactions.<sup>169–171</sup> The Pd-based catalysts reported since 1979 by Suzuki and coworkers consist of molecular complexes of Pd(II) with acetates and phosphine as ligands. The precatalyst initially undergoes reductive elimination to generate the active catalyst in the form of Pd(0) and neutral ligands.<sup>170,172</sup> Despite the numerous challenges associated with the utilization of the Suzuki–Miyaura cross-coupling catalyst, such as potential deactivation by certain reagents and limited reactivity with a few aryl halides, it has paved the way for further research into related catalysts.<sup>173,174</sup>

Yet another industrially important homogeneous catalysis process that has retained its significance for almost 90 years is the hydroformylation reaction, popularly known as the Oxo process.<sup>175,176</sup> The Oxo process, discovered in 1938 by Otto Roelen, is the main route to long-chain aldehydes and alcohols from terminal alkenes.<sup>175</sup> The original catalyst used is the monohydrotetracarbonyl cobalt(I) complex,

$\text{HCo}(\text{CO})_4$ .<sup>177</sup> Later complexes bearing other ligand systems, such as phosphines anchored on Co and Rh metals, have been found to offer excellent performance, achieving high selectivity.<sup>174–177</sup> The track records of these industrially important homogeneous catalysts that turned the fortunes of many industries have presented hope for the current generation to search for new homogeneous catalysts that would also address energy and climate sustainability issues.

## 8. Recovery and recycling of homogeneous catalysts

The main challenge associated with the use of homogeneous catalysts to date has been the recovery of the catalyst from the final reaction mixture. Generally, the catalyst, the reactant, and the product are all present in one phase. Obviously, industries would want to recover high-value catalysts in each cycle of production and reuse them to contain costs. Homogeneous catalyst recovery is not entirely impossible; a few recovery strategies do exist, while others are emerging, depending on the nature of the catalyst, the properties of the product, and the solvent systems used. Recovery approaches include distillation, extraction, chromatography, heterogenization, membrane separation, and biphasic system technology. These methods are situation-specific; some are applicable in industry, while others are potential remedies to a challenge. Three different catalyst recovery approaches are now described in sections 7.1–7.3.

### 8.1. Catalyst recovery by distillation

Catalyst recovery *via* distillation is suitable for volatile products and thermally stable catalysts.<sup>178–182</sup> This method is efficient and is employed in industry for the removal of certain products, leaving the catalyst behind for reuse. A typical example of an industrial process that uses the distillation approach to recover catalysts successfully is the Takasago International Corporation's (–)-menthol synthesis from myrcene.<sup>183</sup> The homogeneous Ru-BINAP catalyst used by Takasago International Corporation (Japan) is usually recovered as a precipitate after the distillation of (–)-menthol from the final reaction mixture.<sup>183</sup> Another example of product distillation from the catalyst is in the Cativa process, where the product and the residual gases are distilled from the catalyst, and the residual gases are recycled back into the reactor.<sup>184</sup> On a laboratory scale, several instances of catalyst recovery by distillation have been reported.<sup>184–186</sup> As mentioned earlier, a challenge sometimes encountered is the volatility of the product. High-boiling-point products require high-temperature conditions, which must be balanced by the thermal stability of the catalyst. Horváth's group demonstrated the complete distillation of  $\gamma$ -valerolactone from Shvo's catalyst, then enabling the recycling of the catalyst four times.<sup>185</sup>  $\gamma$ -Valerolactone has a high boiling point of approximately 207 °C.<sup>186</sup> The practicality of catalyst



recovery from  $\gamma$ -valerolactone was further studied by Amenuvor *et al.*<sup>187</sup> who successfully distilled the product completely from a Ru/Zn cluster catalyst six times, after each cycle, without any significant loss of catalyst activity. These works have demonstrated the industrial applicability of the recovery and reuse of robust catalysts in the biorefinery industry.

To improve energy efficiency and minimize waste, reactive distillation (RD) technology is currently employed in some industries for catalyst recovery.<sup>188,189</sup> In this case, the catalytic reaction and distillation processes are designed as a single unit, and as the product is formed, it is quickly removed by distillation. This technique also enhances product yield and selectivity by decreasing the concentration of the product in the reaction mixture. Thus, RD is very useful here for those reactions that require certain reactants in excess or in rate-limiting reactions.<sup>188,190</sup> Although the RD technology requires improvement in terms of its relatively intricate design and operation,<sup>190</sup> it has been successfully used in several processes, including the production of methyl acetate, methyl *tert*-butyl ether, and *tert*-amyl methyl ether, which are used as additives.<sup>189</sup>

## 8.2. Catalyst recovery using biphasic systems

The biphasic system offers another ingenious approach to homogeneous catalyst recovery from the final reaction mixture. This technique takes advantage of the distribution of the catalyst and product between two immiscible solvents (generally water and an organic solvent). Biphasic catalysis has found industrial application over the past three decades,

with the first appearance being the hydroformylation of propylene to *n*-butyraldehyde by Ruhrchemie AG, Germany.<sup>178,191</sup> One of the basic requirements that makes the biphasic system efficient is the ability of the catalyst to be water-soluble, achieved by making use of water-soluble ligands. The ligand used by Ruhrchemie AG was TPPTS in the form of a Rh catalyst [HRh(CO)(TPPTS)<sub>3</sub>], developed by Rhône-Poulenc, France.<sup>178</sup> TPPTS was further extended to catalyzing the telomerization of dienes and hydrocyanation of olefins using Pd and Ni, respectively.<sup>178</sup> Following this was the introduction of a series of sulfonated phosphine ligands such as BINAS, NAPHOS, NORBOS, and BISBIS, as shown in Fig. 21.<sup>192,193</sup>

The main challenge encountered with water-soluble phosphine ligands is the complexity of their syntheses and the required purification. For instance, attempts to synthesize trisulfonated phosphine ligands usually result in byproducts such as monosulfonated and disulfonated analogues. Some of these impurities remain in the desired ligand even after purification.<sup>178</sup> These earlier works stimulated the expansion of research in the area, focusing on other water-soluble ligands and a special group of ionic liquids that are immiscible with some organic solvents.<sup>194–197</sup> Because of the difficulties in obtaining water-soluble metal catalysts, researchers have been considering immiscible organic solvents that discriminate the solubilities of both the catalyst and the product.<sup>198–200</sup> This eliminates the special design of catalysts for the sake of solubility, since most metal catalysts dissolve in polar organic solvents. The catalyst preferably remains in the polar organic phase while the product moves into the nonpolar organic phase. The Shell

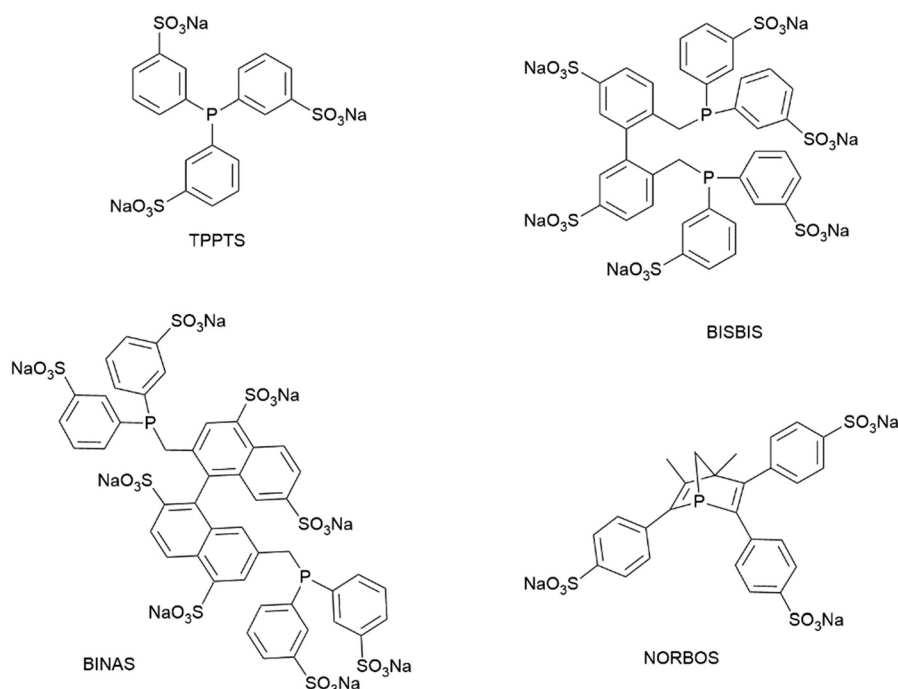


Fig. 21 Examples of ligands used in biphasic catalysis.<sup>162</sup>



higher olefin process (SHOP) for the commercial production of high  $\alpha$ -olefins ( $C_6$ – $C_{20}$ ) is the oldest successful biphasic catalysis carried out using a transition metal complex  $[Ni(COD)Ph_2PCH_2COO]$ .<sup>182,195,200</sup> The catalyst, generated *in situ* from  $NiCl_2$ ,  $Ph_2PCH_2COOH$ , COD, and sodium borohydride as a reducing agent, is soluble in 1,4-butanediol, while the olefin products are not.<sup>195,200</sup> This creates a perfect organic–organic biphasic system where the product serves as one phase and 1,4-butanediol as the other phase.

### 8.3. Catalyst recovery by membrane filtration

A new technique for the separation of homogeneous catalysts and products is organic solvent nanofiltration (OSN). In OSN, use is made of organic solvent-stable membranes that allow separation based on molecular weight differences and branching or bulkiness of side groups.<sup>201–204</sup> Generally, the membrane allows small molecular products to pass through while retaining the catalyst, which is recycled back into the reactor.

This favors catalysts with large molecular weight ligands, such as triphenylphosphine and its derivatives.<sup>201,203</sup> Ideally, one would prefer to make use of OSN rather than traditional methods of distillation because OSN is more selective and the energy demand is lower, leading to cost savings and the preservation of catalyst stability.<sup>205,206</sup> However, research is still ongoing in efforts to overcome its complexity, including the prediction of membrane–solvent behavior, modulation of membrane pore size relative to the sizes of components in mixtures to be separated, feed concentration, temperature considerations, and transmembrane pressure.<sup>202,207–211</sup>

Notwithstanding these challenges, the OSN technique still has the potential to improve homogeneous catalysis. OSN has been used industrially by Exxon Mobil Corporation (USA) and W.R. Grace (USA) in solvent lube dewaxing with an energy cost saving of  $\sim 20\%$ .<sup>212</sup>

Interesting work has been carried out by Janssen *et al.*<sup>203</sup> to develop an in-house engineered continuous flow nanofiltration reactor for the hydroformylation of 1-octene. Using a robust Rh catalyst based on a sterically bulky and rigid phosphine ligand, the system was able to retain  $>99\%$  of the Rh catalyst after 13 days of operation, whilst maintaining very high conversions. There are several more reports of other laboratory-scale investigations involving the use of the OSN strategy for the separation of products from homogeneous catalysts.<sup>207,213–215</sup> Looking ahead, OSN could become the future most preferred method for homogeneous catalyst recovery once the main challenges associated with it are resolved.

## 9. Conclusion – remaining challenges and recommendations

The homogeneously catalyzed (de)hydrogenation of LOHCs, particularly homocyclic and heterocyclic systems, has seen remarkable advancements in recent years. The development

of transition metal-based catalysts with tailored ligands has enhanced the efficiency, selectivity, and sustainability of LOHC (de)hydrogenation processes. Moreover, the exploration of heteroaromatic LOHCs has expanded the potential of LOHC technologies, offering improved hydrogen storage capacity and favorable thermodynamics.

This review highlights the recent advances in the homogeneously catalyzed (de)hydrogenation of LOHCs, as well as challenges related to the industrial application of homogeneous catalysis, including catalyst recovery and reuse. LOHCs present a promising pathway for efficient energy storage and safe hydrogen transportation, which is very critical in the transition to a sustainable hydrogen economy. However, despite rapid progress, several key challenges must be addressed to facilitate the practical deployment of the LOHC technology.

One of the primary challenges lies in the compatibility of heteroaromatic LOHCs with existing energy infrastructure. Many heteroaromatic LOHCs are solid at ambient conditions, posing logistical challenges for storage and transportation. To meet the ideal LOHC criteria, both hydrogen-rich and hydrogen-lean states should exist in the liquid phase. Among the examined *N*-heterocyclic compounds, some quinoline and indole derivatives meet this requirement, coupled with a high hydrogen storage capacity ranging between 5.2 and 7.2 wt%. However, their widespread adoption is hindered by high dehydrogenation enthalpies and toxicity concerns, which limit their practicality in the LOHC technology.

Another major limitation is the efficiency of homogeneous catalytic systems for industrial applications, which is constrained by catalyst stability, cost, and recyclability. Homogeneous hydrogenation processes frequently yield partially hydrogenated products, and when full hydrogenation is achieved, the product selectivity often remains suboptimal, reducing the overall hydrogen storage capacity. Furthermore, the recovery and reuse of homogeneous catalysts in large-scale industrial applications remain challenging, adding to operational costs and sustainability concerns.

Furthermore, in homogeneous catalysis LOHCs, the hydrogen-to-substrate (H/S) ratio is a fundamental metric that integrates both the theoretical storage capacity of the carrier, and the practical demands placed on the catalytic cycle. The H/S ratio describes the number of hydrogen equivalents that can be chemically bound per molecule of the substrate during complete hydrogenation; this directly defines the gravimetric hydrogen storage capacity (wt%  $H_2$ ), a primary target for LOHC technologies. For example, *N*-ethylcarbazole (NEC), one of the most studied LOHC candidates, can be fully hydrogenated to dodecahydro-NEC by uptake of six equivalents of  $H_2$ , corresponding to an ideal capacity of  $\sim 5.8$  wt%  $H_2$ , a level that approaches practical benchmarks for hydrogen carriers. Achieving and sustaining a high effective H/S ratio in practice hinges on catalyst performance across multiple sequential hydrogenation steps. Homogeneous catalysts, with their tunable ligand



environments and capability to mediate H–H activation under milder conditions than many heterogeneous systems, offer a route to drive hydrogenation efficiently toward fully saturated LOHC states. However, this same requirement underscores a key challenge: catalysts must maintain activity and selectivity through the entire sequence of hydrogen additions, not only in early steps—otherwise the system stalls at partial hydrogenation and the realized H/S ratio falls below theoretical values. Moreover, the H/S ratio is tightly coupled to operational and system considerations. High H/S ratios necessitate catalysts capable of handling elevated hydrogen pressures and multiple turnovers without degradation, and they influence reactor design, mass transfer, and thermodynamics; incomplete attainment of the target H/S ratio decreases the effective hydrogen density and compromises cyclic reversibility. In this context, homogeneous catalyst designs that can sustain high conversion and selectivity across full hydrogenation–dehydrogenation cycles are critical for translating LOHC chemistry into practical hydrogen storage media.

Additionally, rational catalyst design has yet to fully integrate computational methodologies. Advanced computational modelling and mechanistic studies could significantly enhance catalyst development, enabling the targeted design of more stable, efficient, and selective catalytic systems. The synergy between experimental and theoretical approaches can accelerate breakthroughs in LOHC technology.

In conclusion, recommendations for future research should include the following. Looking ahead, research should focus on developing new LOHC systems that can meet the US DOE's requirements. Additionally, priority should be placed on rational catalyst design, incorporating computational methods, and bridging the gap between laboratory-scale innovations and large-scale implementations. Further, advancing the understanding of structure–activity relationships in catalysis, along with innovations in green chemistry, can also promote the sustainable and widespread adoption of LOHC technologies.

Research advancements have revealed that in some homogeneous (de)hydrogenation reactions, the true active species are *in situ*-generated soluble metal nanoclusters or colloidal nanoparticles (NPs). These species often exhibit high catalytic activity, even for challenging substrates. For instance, the full hydrogenation of quinoline to DHQ has been challenging with homogeneous catalysts alone. However, recent studies indicate that dual catalysis, where a molecular complex facilitates heteroarene hydrogenation while *in situ*-generated Ru NPs promote arene hydrogenation, can achieve this transformation. The stabilization of such NPs and clusters by ligands, additives, and/or solvents leads to hybrid catalytic systems that integrate features of both homogeneous and heterogeneous catalysis. The rational design of these hybrid catalysts represents a promising avenue for enhancing LOHC technology and improving its industrial viability.

By addressing these challenges, the future of LOHC systems holds immense promise for advancing the hydrogen economy and achieving sustainable energy solutions. Continued research efforts in catalyst innovation, process optimization, and computational modelling will be critical in realizing the full potential of LOHCs as a cornerstone of next-generation energy storage and hydrogen transport technologies.

## Author contributions

Juliana Mana Edor: writing – original draft, review & editing. Gershon Amenuvor: writing – original draft, review & editing. Phillimon Modisha: writing – review & editing, and supervision. Dmitri Bessarabov: conceptualization and resources.

## Conflicts of interest

There are no conflicts to declare.

## Data availability

No primary research results, software, or code have been included, and no new data were generated or analysed as part of this review.

## Acknowledgements

We are grateful to the North-West University, Hydrogen South Africa (HySA Infrastructure CoC), and the Kwame Nkrumah University of Science and Technology for their support.

## References

- 1 T.-H. Le, N. Tran and H.-J. Lee, Development of Liquid Organic Hydrogen Carriers for Hydrogen Storage and Transport, *Int. J. Mol. Sci.*, 2024, **25**, 1359.
- 2 V. Tietze, S. Luhr and D. Stolten, Bulk Storage Vessels for Compressed and Liquid Hydrogen, In *Hydrogen Science and Engineering: Materials, Processes, Systems and Technology*, ed. D. Stolten and B. Emonts, Wiley, 2016, pp. 659–690.
- 3 A. Alekseev, Hydrogen Liquefaction, In *Hydrogen Science and Engineering: Materials, Processes, Systems and Technology*, ed. D. Stolten and B. Emonts, Wiley, 2016, pp. 733–762.
- 4 S. J. Wang, Z. Y. Zhang, Y. Tan, K. X. Liang and S. H. Zhang, Review on the characteristics of existing hydrogen energy storage technologies, *Energy Sources, Part A*, 2023, **45**, 985.
- 5 S. Satyapal, J. Petrovic, C. Read, G. Thomas and G. Ordaz, The U.S. Department of Energy's National Hydrogen Storage Project: Progress towards Meeting Hydrogen-Powered Vehicle Requirements, *Catal. Today*, 2007, **120**, 246.
- 6 Z. Wang, I. Tonks, J. Belli and C. M. Jensen, Dehydrogenation of N-Ethyl Perhydrocarbazole Catalyzed by



- PCP Pincer Iridium Complexes: Evaluation of a Homogeneous Hydrogen Storage System, *J. Organomet. Chem.*, 2009, **694**, 2854.
- 7 A. Ali, M. Usman, H. M. Ali, U. Sajjad, Md. A. Aziz and M. N. Shaikh, Bayesian surrogate assisted neural network model to predict the hydrogen storage in 9-ethylcarbazole, *Int. J. Thermofluids*, 2025, **27**, 101270.
  - 8 J.-Y. Cho, H. Kim, J.-E. Oh and B. Y. Park, Recent Advances in Homogeneous/Heterogeneous Catalytic Hydrogenation and Dehydrogenation for Potential Liquid Organic Hydrogen Carrier (LOHC) Systems, *Catalysts*, 2021, **11**, 1497.
  - 9 P. M. Modisha, C. N. M. Ouma, R. Garidzirai, P. Wasserscheid and D. Bessarabov, The Prospect of Hydrogen Storage Using Liquid Organic Hydrogen Carriers, *Energy Fuels*, 2019, **33**, 2778.
  - 10 P. Modisha, P. Gqogqa, R. Garidzirai, C. N. M. Ouma and D. Bessarabov, Evaluation of Catalyst Activity for Release of Hydrogen from Liquid Organic Hydrogen Carriers, *Int. J. Hydrogen Energy*, 2019, **44**, 21926.
  - 11 P. Modisha, R. Garidzirai, H. Güneş, S. E. Bozbag, S. Rommel, E. Uzunlar, M. Aindow, C. Erkey and D. Bessarabov, A Promising Catalyst for the Dehydrogenation of Perhydro-Dibenzyltoluene: Pt/Al<sub>2</sub>O<sub>3</sub> Prepared by Supercritical CO<sub>2</sub> Deposition, *Catalysts*, 2022, **12**, 489.
  - 12 J. M. Eder, M. C. Joseph, J. H. L. Jordaan, H. C. M. Vosloo and A. J. Swarts, Formic Acid Dehydrogenation Catalysis Using Novel Pyridyl-Formamidine Half-Sandwich Ruthenium(II) Complexes, *Appl. Organomet. Chem.*, 2025, **39**, e70016.
  - 13 P. Bachmann, J. Steinhauer, F. Späth, F. Düll, U. Bauer, R. Eschenbacher, F. Hemauer, M. Scheuermeyer, A. Bösmann, M. Büttner, C. Neiß, A. Görling, P. Wasserscheid, H.-P. Steinrück and C. Papp, Dehydrogenation of the Liquid Organic Hydrogen Carrier System 2-Methylindole/2-Methylindoline/2-Methyloctahydroindole on Pt(111), *J. Chem. Phys.*, 2019, **151**, 144711.
  - 14 K. C. Tan, Y. S. Chua, T. He and P. Chen, Strategies of Thermodynamic Alternation on Organic Hydrogen Carriers for Hydrogen Storage Application: A Review, *Green Energy Resour.*, 2023, **1**, 100020.
  - 15 Q. Du, L. Liu and T. Zhou, General and Efficient Copper-Catalyzed Oxazaborolidine Complex in Transfer Hydrogenation of Isoquinolines under Mild Conditions, *ACS Omega*, 2020, **5**, 21219.
  - 16 N. Brückner, K. Obesser, A. Bösmann, D. Teichmann, W. Arlt, J. Dungs and P. Wasserscheid, Evaluation of Industrially Applied Heat-Transfer Fluids as Liquid Organic Hydrogen Carrier Systems, *ChemSusChem*, 2014, **7**, 229.
  - 17 H. S. Alghamdi, A. Ali, A. M. Ajeebi, A. Jedidi, M. Sanhoob, M. Aktary, A. H. Shabi, M. Usman, W. Alghamdi, S. Alzahrani, Md. A. Aziz and M. N. Shaikh, Catalysts for Liquid Organic Hydrogen Carriers (LOHCs): Efficient Storage and Transport for Renewable Energy, *Chem. Rec.*, 2024, **24**, e202400082.
  - 18 D. Wei, X. Shi, R. Qu, K. Junge, H. Junge and M. Beller, Toward a Hydrogen Economy: Development of Heterogeneous Catalysts for Chemical Hydrogen Storage and Release Reactions, *ACS Energy Lett.*, 2022, **7**, 3734.
  - 19 Y. Zhang, J. Wang, F. Zhou and J. Liu, An effective strategy for hydrogen supply: catalytic acceptorless dehydrogenation of N-heterocycles, *Catal. Sci. Technol.*, 2021, **11**, 3990.
  - 20 Y. Li, X. Guo, S. Zhang and Y. A. He, Perspective Review on N-Heterocycles as Liquid Organic Hydrogen Carriers and Their Hydrogenation/Dehydrogenation Catalysts, *Energy Fuels*, 2024, **38**, 12447.
  - 21 T. Yamada, K. Park and H. Sajiki, Homogeneously Catalyzed Aromatic Reduction, In *Industrial Arene Chemistry: Markets, Technologies, Sustainable Processes and Case Studies of Aromatic Commodities*, ed. J. Mortier and M. Maas-Brunner, Wiley-VCH, Weinheim, 2023, pp. 849–881.
  - 22 A. Lin and G. Bagnato, Revolutionising energy storage: The Latest Breakthrough in liquid organic hydrogen carriers, *Int. J. Hydrogen Energy*, 2024, **63**, 315.
  - 23 A. Kumar, T. Janes, N. A. Espinosa-Jalapa and D. Milstein, Selective Hydrogenation of Cyclic Imides to Diols and Amines and Its Application in the Development of a Liquid Organic Hydrogen Carrier, *J. Am. Chem. Soc.*, 2018, **140**, 7453.
  - 24 Y. Xie, P. Hu, Y. Ben-David and D. Milstein, A Reversible Liquid Organic Hydrogen Carrier System Based on Methanol-Ethylenediamine and Ethylene Urea, *Angew. Chem., Int. Ed.*, 2019, **58**, 5105.
  - 25 B. Loges, A. Boddien, H. Junge and M. Beller, Controlled Generation of Hydrogen from Formic Acid Amine Adducts at Room Temperature and Application in H<sub>2</sub>/O<sub>2</sub> Fuel Cells, *Angew. Chem., Int. Ed.*, 2008, **47**, 3962.
  - 26 D. R. Palo, R. A. Dagle and J. D. Holladay, Methanol Steam Reforming for Hydrogen Production, *Chem. Rev.*, 2007, **107**, 3992.
  - 27 T. He, Q. Pei and P. Chen, Liquid Organic Hydrogen Carriers, *J. Energy Chem.*, 2015, **24**, 587.
  - 28 T. Shimabayashi and K. Fujita, Metal-Catalyzed Hydrogenation and Dehydrogenation Reactions for Efficient Hydrogen Storage, *Tetrahedron*, 2020, **76**, 130946.
  - 29 C. J. Boxwell, P. J. Dyson, D. J. Ellis and T. Welton, A Highly Selective Arene Hydrogenation Catalyst That Operates in Ionic Liquid, *J. Am. Chem. Soc.*, 2002, **124**, 9334.
  - 30 V. Arun, N. Sridevi, P. P. Robinson, S. Manju and K. K. M. Yusuff, Ni(II) and Ru(II) Schiff Base Complexes as Catalysts for the Reduction of Benzene, *J. Mol. Catal. A:Chem.*, 2009, **304**, 191.
  - 31 C. Vangelis, A. Bouriazos, S. Sotiriou, M. Samorski, B. Gutsche and G. Papadogianakis, Catalytic Conversions in Green Aqueous Media: Highly Efficient Biphasic Hydrogenation of Benzene to Cyclohexane Catalyzed by Rh/TPPTS Complexes, *J. Catal.*, 2010, **274**, 21.
  - 32 J. Meng, F. Zhou, H. Ma, X. Yuan, Y. Wang and J. A. Zhang, Review of Catalysts for Methylcyclohexane Dehydrogenation, *Top. Catal.*, 2021, **64**, 509.



- 33 H.-L. Ye, S.-X. Liu, C. Zhang, Y.-Q. Cai and Y.-F. Shi, Dehydrogenation of Methylcyclohexane over Pt-Based Catalysts Supported on Functional Granular Activated Carbon, *RSC Adv.*, 2021, **11**, 29287.
- 34 S. Yolcular and Ö. Olgun, Hydrogen Storage in the Form of Methylcyclohexane, *Energy Sources, Part A*, 2007, **30**, 149.
- 35 P. Gupta, G. Hierlmeier, C. Baete, M. V. Pecoraro, P. Tosatti, K. Puentener and P. J. Chirik, Asymmetric Hydrogenation of Naphthalenes with Molybdenum Catalysts: Ligand Design Improves Chemoselectivity, *ACS Catal.*, 2024, **14**, 15545.
- 36 S. Hodoshima, H. Arai, S. Takaiwa and Y. Saito, Catalytic decalin Dehydrogenation/Naphthalene Hydrogenation Pair as a Hydrogen Source for Fuel-Cell Vehicle, *Int. J. Hydrogen Energy*, 2003, **28**, 1255.
- 37 Y. Tuo, L. Yang, H. Cheng, M. Yang, Y.-A. Zhu and P. Li, Density Functional Theory Study of Decalin Dehydrogenation for Hydrogen Release on Pt(111) and Pt(211), *Int. J. Hydrogen Energy*, 2018, **43**, 19575.
- 38 L. M. Kustov, A. L. Tarasov and B. P. Tarasov, Intermetallide Catalysts for Hydrogen Storage on the Basis of Reversible Aromatics Hydrogenation/Dehydrogenation Reactions, *Int. J. Hydrogen Energy*, 2013, **38**, 5713.
- 39 M. Kerscher, T. Klein, P. S. Schulz, E. Veroutis, S. Dürr, P. Preuster, T. M. Koller, M. H. Rausch, I. G. Economou, P. Wasserscheid and A. P. Fröba, Thermophysical Properties of Diphenylmethane and Dicyclohexylmethane as a Reference Liquid Organic Hydrogen Carrier System from Experiments and Molecular Simulations, *Int. J. Hydrogen Energy*, 2020, **45**, 28903.
- 40 D. J. Han, Y. S. Jo, B. S. Shin, M. Jang, J. W. Kang, J. H. Han, S. W. Nam and C. W. Yoon, A Novel Eutectic Mixture of Biphenyl and Diphenylmethane as a Potential Liquid Organic Hydrogen Carrier: Catalytic Hydrogenation, *Energy Technol.*, 2019, **7**, 113.
- 41 B. Bong, C. Mebrahtu, D. Jurado, A. Bösmann, P. Wasserscheid and R. Palkovits, Hydrogen Loading and Release Potential of the LOHC System Benzyltoluene/Perhydro Benzyltoluene over S-Pt/TiO<sub>2</sub> Catalyst, *ACS Eng. Au*, 2024, **4**, 359.
- 42 D. Strauch, P. Weiner, B. B. Sarma, A. Körner, E. Herzinger, P. Wolf, A. Zimina, A. Hutzler, D. E. Doronkin, J.-D. Grunwaldt, P. Wasserscheid and M. Wolf, Bimetallic Platinum Rhenium Catalyst for Efficient Low Temperature Dehydrogenation of Perhydro Benzyltoluene, *Catal. Sci. Technol.*, 2024, **14**, 1775.
- 43 A. Leinweber and K. Müller, Hydrogenation of the Liquid Organic Hydrogen Carrier Compound Monobenzyl Toluene: Reaction Pathway and Kinetic Effects, *Energy Technol.*, 2018, **6**, 513.
- 44 R. Garidzirai, P. Modisha, I. Shuro, J. Visagie, P. Van Helden and D. Bessarabov, The Effect of Mg and Zn Dopants on Pt/Al<sub>2</sub>O<sub>3</sub> for the Dehydrogenation of Perhydrodibenzyltoluene, *Catalysts*, 2021, **11**, 490.
- 45 P. Modisha and D. Bessarabov, Stress Tolerance Assessment of Dibenzyltoluene-Based Liquid Organic Hydrogen Carriers, *Sustainable Energy Fuels*, 2020, **4**, 4662.
- 46 A. N. Kalenchuk and L. M. Kustov, Activity of Mono-, Bi-, and Trimetallic Catalysts Pt-Ni-Cr/C in the Bicyclohexyl Dehydrogenation Reaction, *Molecules*, 2022, **27**, 8416.
- 47 L. M. Kustov and A. N. Kalenchuk, Effect of Cr on a Ni-Catalyst Supported on Sibunite in Bicyclohexyl Dehydrogenation in Hydrogen Storage Application, *Catalysts*, 2022, **12**, 1506.
- 48 A. N. Kalenchuk, V. I. Bogdan, S. F. Dunaev and L. M. Kustov, Effect of Surface Hydrophilization on Pt/Sibunit Catalytic Activity in Bicyclohexyl Dehydrogenation in Hydrogen Storage Application, *Int. J. Hydrogen Energy*, 2018, **43**, 6191.
- 49 C. Chu, K. Wu, B. Luo, Q. Cao and H. Zhang, Hydrogen Storage by Liquid Organic Hydrogen Carriers: Catalyst, Renewable Carrier, and Technology – A Review, *Carbon Resour. Convers.*, 2023, **6**, 334.
- 50 R. Biniwale, S. Rayalu, S. Devotta and M. Ichikawa, Chemical Hydrides: A Solution to High Capacity Hydrogen Storage and Supply, *Int. J. Hydrogen Energy*, 2008, **33**, 360.
- 51 G. P. Pez, A. R. Scott, A. C. Cooper and H. Cheng, Hydrogen storage by reversible hydrogenation of pi-conjugated substrates, US7101530B2, September 5, 2006, <https://patents.google.com/patent/US7101530B2/en>, (Accessed 2025-03-10).
- 52 Q.-L. Zhu and Q. Xu, Liquid Organic and Inorganic Chemical Hydrides for High-Capacity Hydrogen Storage, *Energy Environ. Sci.*, 2015, **8**, 478.
- 53 E. Díaz, P. Rapado-Gallego and S. Ordonez, Systematic evaluation of physicochemical properties for the selection of alternative liquid organic hydrogen carriers, *J. Energy Storage*, 2023, **59**, 106511.
- 54 B. S. Shin, C. W. Yoon, S. K. Kwak and J. W. Kang, Thermodynamic assessment of carbazole-based organic polycyclic compounds for hydrogen storage applications via a computational approach, *Int. J. Hydrogen Energy*, 2018, **43**, 12158.
- 55 E. Farnetti, R. D. Monte and J. Kašpar, *Homogeneous and Heterogeneous Catalysis*, Eolss Publishers, Oxford, UK, 2009, vol. 2, p. 502.
- 56 T. Suárez, A. Guzmán, B. Fontal, M. Reyes, F. Bellandi, R. R. Contreras, P. Cancines, G. León and L. Rojas, Hydrogenation of Aromatics with [Ru( $\eta^5$ -C<sub>5</sub>H<sub>5</sub>)Cl(PPDS)]<sub>2</sub> in Biphasic Medium, *Transition Met. Chem.*, 2006, **31**, 176.
- 57 P. J. Dyson, D. J. Ellis and G. Laurenczy, Minor Modifications to the Ligands Surrounding a Ruthenium Complex Lead to Major Differences in the Way in Which They Catalyse the Hydrogenation of Arenes, *Adv. Synth. Catal.*, 2003, **345**, 211.
- 58 A. F. Borowski, L. Vendier, S. Sabo-Etienne, E. Rozycka-Sokolowska and A. V. Gaudyn, Catalyzed Hydrogenation of Condensed Three-Ring Arenes and Their N-Heteroaromatic Analogues by a Bis(Dihydrogen) Ruthenium Complex, *Dalton Trans.*, 2012, **41**, 14117.
- 59 B. Chatterjee, D. Kalsi, A. Kaithal, A. Bordet, W. Leitner and C. Gunanathan, One-Pot Dual Catalysis for the



- Hydrogenation of Heteroarenes and Arenes, *Catal. Sci. Technol.*, 2020, **10**, 5163.
- 60 E. L. Muetterties and F. J. Hirsekorn, Homogeneous Catalysis of Aromatic Hydrocarbon Hydrogenation Reactions, *J. Am. Chem. Soc.*, 1974, **96**, 4063.
- 61 P. J. Dyson, Arene Hydrogenation by Homogeneous Catalysts: Fact or Fiction?, *Dalton Trans.*, 2003, 2964.
- 62 I. P. A. Rothwell, New Generation of Homogeneous Arene Hydrogenation Catalysts, *Chem. Commun.*, 1997, 1331.
- 63 M. V. Joannou, M. J. Bezdek and P. J. Chirik, Pyridine(Diimine) Molybdenum-Catalyzed Hydrogenation of Arenes and Hindered Olefins: Insights into Precatalyst Activation and Deactivation Pathways, *ACS Catal.*, 2018, **8**, 5276.
- 64 G. Hierlmeier, P. Tosatti, K. Puentener and P. J. Chirik, Identification of Cyclohexadienyl Hydrides as Intermediates in Molybdenum-Catalyzed Arene Hydrogenation, *Angew. Chem.*, 2023, **135**, e202216026.
- 65 P. Viereck, G. Hierlmeier, P. Tosatti, T. P. Pabst, K. Puentener and P. J. Chirik, Molybdenum-Catalyzed Asymmetric Hydrogenation of Fused Arenes and Heteroarenes, *J. Am. Chem. Soc.*, 2022, **144**, 11203.
- 66 K. J. Klabunde, B. B. Anderson, M. Bader and L. J. Radonovich,  $\Pi$ -Arene Complexes of Nickel(II) Stabilized by Sigma-Bonded pentafluorophenyl Ligands. Homogeneous Arene Hydrogenation Catalysis and Unusually Labile  $\Pi$ -Arene Ligands, *J. Am. Chem. Soc.*, 1978, **100**, 1313.
- 67 A. Gómez-Torres, J. R. Aguilar-Calderón, A. M. Encerrado-Manriquez, M. Pink, A. J. Metta-Magaña, W. Lee and S. Fortier, Titanium-Mediated Catalytic Hydrogenation of Monocyclic and Polycyclic Arenes, *Chem. – Eur. J.*, 2020, **26**, 2803.
- 68 B. Han, P. Ma, X. Cong, H. Chen and X. Zeng, Chromium- and Cobalt-Catalyzed, Regiocontrolled Hydrogenation of Polycyclic Aromatic Hydrocarbons: A Combined Experimental and Theoretical Study, *J. Am. Chem. Soc.*, 2019, **141**, 9018.
- 69 R. Johnson, P. Hu, J. Pugh, R. K. Haridasan and K. Searles, Benzene Hydrogenation Utilizing Organometallic Early Transition Metal Precursors, *Catal. Sci. Technol.*, 2025, **15**, 41.
- 70 C. M. Jensen, Iridium PCP Pincer Complexes: Highly Active and Robust Catalysts for Novel Homogeneous Aliphatic Dehydrogenations, *Chem. Commun.*, 1999, **24**, 2443.
- 71 C. M. Jensen, Hydrogen storage, US6074447A, June 13, 2000, <https://patents.google.com/patent/US6074447A/en>, (Accessed on 2025-03-10).
- 72 J. Zheng, H. Zhou, C.-G. Wang, E. Ye, J. W. Xu, X. J. Loh and Z. Li, Current Research Progress and Perspectives on Liquid Hydrogen Rich Molecules in Sustainable Hydrogen Storage, *Energy Storage Mater.*, 2021, **35**, 695.
- 73 S. P. Verevkin, S. P. Safronov, A. A. Samarov and S. V. Vostrikov, Hydrogen Storage: Thermodynamic Analysis of Alkyl-Quinolines and Alkyl-Pyridines as Potential Liquid Organic Hydrogen Carriers (LOHC), *Appl. Sci.*, 2021, **11**, 11758.
- 74 M. Zhou, Y. Miao, Y. Gu and Y. Xie, Recent Advances in Reversible Liquid Organic Hydrogen Carrier Systems: From Hydrogen Carriers to Catalysts, *Adv. Mater.*, 2024, **36**, 2311355.
- 75 Y. Luo, X. Yue, P. Wei, A. Zhou, X. Kong and S. Alimzhanova, A State-of-the-Art Review of Quinoline Degradation and Technical Bottlenecks, *Sci. Total Environ.*, 2020, **747**, 141136.
- 76 Y.-N. Duan, X. Du, Z. Cui, Y. Zeng, Y. Liu, T. Yang, J. Wen and X. Zhang, Homogeneous Hydrogenation with a Cobalt/Tetraphosphine Catalyst: A Superior Hydride Donor for Polar Double Bonds and N-Heteroarenes, *J. Am. Chem. Soc.*, 2019, **141**, 20424.
- 77 T. Vielhaber, C. Heizinger and C. Topf, Homogeneous Pressure Hydrogenation of Quinolines Effected by a Bench-Stable Tungsten-Based Pre-Catalyst, *J. Catal.*, 2021, **404**, 451.
- 78 K. Michaliszyn, E. S. Smirnova, A. Bucci, V. Martin-Diaconescu and J. Lloret Fillol, Well-defined Nickel P3C Complexes as Hydrogenation Catalysts of N-Heteroarenes Under Mild Conditions, *ChemCatChem*, 2022, **14**, e202200039.
- 79 V. Papa, J. Fessler, F. Zaccaria, J. Hervochon, P. Dam, C. Kubis, A. Spannenberg, Z. Wei, H. Jiao, C. Zuccaccia, A. Macchioni, K. Junge and M. Beller, Efficient Hydrogenation of N-Heterocycles Catalyzed by NNP–Manganese(I) Pincer Complexes at Ambient Temperature, *Chem. – Eur. J.*, 2023, **29**, e202202774.
- 80 R. Kumar, M. K. Pandey, A. Bhandari and J. Choudhury, Balancing the Seesaw in Mn-Catalyzed N-Heteroarene Hydrogenation: Mechanism-Inspired Catalyst Design for Simultaneous Taming of Activation and Transfer of H<sub>2</sub>, *ACS Catal.*, 2023, **13**, 4824.
- 81 R. Kumar, M. K. Pandey, I. K. Pandey, A. Kumar and J. Choudhury, An Imidazolyidene-Based Mesoionic Carbene–Mn(I) Complex and Its Catalytic Potential in N-Heteroarene Hydrogenation, *Eur. J. Inorg. Chem.*, 2023, **26**, e202300411.
- 82 G. E. Dobereiner, A. Nova, N. D. Schley, N. Hazari, S. J. Miller, O. Eisenstein and R. H. Crabtree, Iridium-Catalyzed Hydrogenation of N-Heterocyclic Compounds under Mild Conditions by an Outer-Sphere Pathway, *J. Am. Chem. Soc.*, 2011, **133**, 7547.
- 83 D. Wang and D. Astruc, The Golden Age of Transfer Hydrogenation, *Chem. Rev.*, 2015, **115**, 6621.
- 84 S. Werkmeister, J. Neumann, K. Junge and M. Beller, Pincer-Type Complexes for Catalytic (De)Hydrogenation and Transfer (De)Hydrogenation Reactions: Recent Progress, *Chem. – Eur. J.*, 2015, **21**, 12226.
- 85 Y. Wang, B. Dong, Z. Wang, X. Cong and X. Bi, Silver-Catalyzed Reduction of Quinolines in Water, *Org. Lett.*, 2019, **21**, 3631.
- 86 M. Zhang, B. Han, H. Ma, L. Zhao, J. Wang and Y. Zhang, Hydrosilanes as Hydrogen Source: Iridium-Catalyzed Hydrogenation of N-Heteroarenes, *Chin. J. Org. Chem.*, 2022, **42**, 1170.



- 87 Y. Watanabe, T. Ohta, Y. Tsuji, T. Hiyoshi and Y. Tsuji, Ruthenium Catalyzed Reduction of Nitroarenes and Azaaromatic Compounds Using Formic Acid, *Bull. Chem. Soc. Jpn.*, 1984, **57**, 2440.
- 88 H. Qi, L. Wang, Q. Sun and W. Sun, Asymmetric Transfer Hydrogenation of Quinoline Derivatives Catalyzed by Chiral Iridium-Imidazoline Complex in Water, *Mol. Catal.*, 2022, **532**, 112715.
- 89 B. Maji and J. Choudhury, Reusable Water-soluble Homogeneous Catalyst in Aqueous-phase Transfer Hydrogenation of N-heteroarenes with Formic Acid: Uracil-based Bifunctional Ir-NHC Catalyst Is the Key, *Appl. Organomet. Chem.*, 2024, **38**, e6720.
- 90 J. R. Cabrero-Antonino, R. Adam, K. Junge, R. Jackstell and M. Beller, Cobalt-Catalysed Transfer Hydrogenation of Quinolines and Related Heterocycles Using Formic Acid under Mild Conditions, *Catal. Sci. Technol.*, 2017, **7**, 1981.
- 91 V. Vermaak, H. C. M. Vosloo and A. J. Swarts, Fast and Efficient Nickel(II)-catalysed Transfer Hydrogenation of Quinolines with Ammonia Borane, *Adv. Synth. Catal.*, 2020, **362**, 5788.
- 92 W.-G. Jia, L.-L. Gao, Z.-B. Wang, J.-J. Wang, E.-H. Sheng and Y.-F. Han, NHC-Palladium(II) Mononuclear and Binuclear Complexes Containing Phenylene-Bridged Bis(Thione) Ligands: Synthesis, Characterization, and Catalytic Activities, *Organometallics*, 2020, **39**, 1790.
- 93 X. Cui, W. Huang and L. Wu, Zirconium-Hydride-Catalyzed Transfer Hydrogenation of Quinolines and Indoles with Ammonia Borane, *Org. Chem. Front.*, 2021, **8**, 5002.
- 94 A. Maji, S. Gupta, D. Panja, S. Sutradhar and S. Kundu, Hydrogenation of N-Heterocycles by a Well-Defined Phosphine-Free Manganese Catalyst Using Ammonia Borane, *Organometallics*, 2023, **42**, 3385.
- 95 T. Bhatt and K. Natte, Transfer Hydrogenation of N- and O-Containing Heterocycles Including Pyridines with H<sub>3</sub>N-BH<sub>3</sub> Under the Catalysis of the Homogeneous Ruthenium Precatalyst, *Org. Lett.*, 2024, **26**, 866.
- 96 W. Mao, D. Song, J. Guo, K. Zhang, C. Zheng, J. Lin, L. Huang, L. Zheng, W. Zhong and F. Ling, Manganese-Catalyzed Asymmetric Transfer Hydrogenation of Quinolines in Water Using Ammonia Borane as a Hydrogen Source, *Green Chem.*, 2024, **26**, 5933.
- 97 X. Chu, G. Zhou, M. Pang and H. Zhang, Manganese-Catalysed Transfer Hydrogenation of Quinolines under Mild Conditions, *Eur. J. Org. Chem.*, 2023, **26**, e202300597.
- 98 K. Fujita, C. Kitatsuji, S. Furukawa and R. Yamaguchi, Regio- and Chemoselective Transfer Hydrogenation of Quinolines Catalyzed by a Cp\*Ir Complex, *Tetrahedron Lett.*, 2004, **45**, 3215.
- 99 R. He, P. Cui, D. Pi, Y. Sun and H. Zhou, High Efficient Iron-Catalyzed Transfer Hydrogenation of Quinolines with Hantzsch Ester as Hydrogen Source under Mild Conditions, *Tetrahedron Lett.*, 2017, **58**, 3571.
- 100 A. Sau, D. Mahapatra, A. Maji, S. Dey, A. Roy and S. Kundu, Methyl Formate, an Alternative Transfer Hydrogenating Agent for Chemoselective Reduction of N-Heteroarenes and Azoarenes, *Org. Lett.*, 2024, **26**, 4486.
- 101 Y. Gong, J. He, X. Wen, H. Xi, Z. Wei and W. Liu, Transfer Hydrogenation of N-Heteroarenes with 2-Propanol and Ethanol Enabled by Manganese Catalysis, *Org. Chem. Front.*, 2021, **8**, 6901.
- 102 M. P. Wiesenfeldt, Z. Nairoukh, T. Dalton and F. Glorius, Selective Arene Hydrogenation for Direct Access to Saturated Carbo- and Heterocycles, *Angew. Chem., Int. Ed.*, 2019, **58**, 10460.
- 103 A. F. Borowski, S. Sabo-Etienne, B. Donnadiou and B. Chaudret, Reactivity of the Bis(Dihydrogen) Complex [RuH<sub>2</sub>(η<sup>2</sup>-H<sub>2</sub>)<sub>2</sub>(PCy<sub>3</sub>)<sub>2</sub>] toward N-Heteroaromatic Compounds. Regioselective Hydrogenation of Acridine to 1,2,3,4,5,6,7,8-Octahydroacridine, *Organometallics*, 2003, **22**, 1630.
- 104 S. Urban, N. Ortega and F. Glorius, Ligand-Controlled Highly Regioselective and Asymmetric Hydrogenation of Quinoxalines Catalyzed by Ruthenium N-Heterocyclic Carbene Complexes, *Angew. Chem., Int. Ed.*, 2011, **50**, 3803.
- 105 R. Kuwano, R. Ikeda and K. Hirasada, Catalytic Asymmetric Hydrogenation of Quinoline Carbocycles: Unusual Chemoselectivity in the Hydrogenation of Quinolines, *Chem. Commun.*, 2015, **51**, 7558.
- 106 Y. Jin, Y. Makida, T. Uchida and R. Kuwano, Ruthenium-Catalyzed Chemo- and Enantioselective Hydrogenation of Isoquinoline Carbocycles, *J. Org. Chem.*, 2018, **83**, 3829.
- 107 C. Luo, C. Wu, X. Wang, Z. Han, Z. Wang and K. Ding, Ruthenium-Catalyzed Carbocycle-Selective Hydrogenation of Fused Heteroarenes, *J. Am. Chem. Soc.*, 2024, **146**, 35043.
- 108 A. P. Koskin, J. Zhang, O. B. Belskaya, O. A. Bulavchenko, D. A. Konovalova, S. A. Stepanenko, A. V. Ishchenko, I. G. Danilova, V. L. Yurpalov, Y. V. Larichev, R. Kukushkin and P. M. Yeletsky, Efficiency of High-Loaded Nickel Catalysts Modified by Mg in Hydrogen Storage/Extraction Using Quinoline/Decahydroquinoline Pair as LOHC Substrates, *J. Magnesium Alloys*, 2024, **12**, 3245.
- 109 R. Yamaguchi, C. Ikeda, Y. Takahashi and K. Fujita, Homogeneous Catalytic System for Reversible Dehydrogenation-Hydrogenation Reactions of Nitrogen Heterocycles with Reversible Interconversion of Catalytic Species, *J. Am. Chem. Soc.*, 2009, **131**, 8410.
- 110 X.-B. Zhang and Z. A. Xi, Theoretical Study of the Mechanism for the Homogeneous Catalytic Reversible Dehydrogenation-Hydrogenation of Nitrogen Heterocycles, *Phys. Chem. Chem. Phys.*, 2011, **13**, 3997.
- 111 H. Li, J. Jiang, G. Lu, F. Huang and Z.-X. Wang, On the "Reverse Gear" Mechanism of the Reversible Dehydrogenation/Hydrogenation of a Nitrogen Heterocycle Catalyzed by a Cp\*Ir Complex: A Computational Study, *Organometallics*, 2011, **30**, 3131.
- 112 M. G. Manas, L. S. Sharninghausen, E. Lin and R. H. Crabtree, Iridium Catalyzed Reversible Dehydrogenation-Hydrogenation of Quinoline Derivatives under Mild Conditions, *J. Organomet. Chem.*, 2015, **792**, 184.



- 113 Á. Vivancos, M. Beller and M. Albrecht, NHC-Based Iridium Catalysts for Hydrogenation and Dehydrogenation of N-Heteroarenes in Water under Mild Conditions, *ACS Catal.*, 2018, **8**, 17.
- 114 S. Wang, H. Huang, C. Bruneau and C. Fischmeister, Iridium-Catalyzed Hydrogenation and Dehydrogenation of N-Heterocycles in Water under Mild Conditions, *ChemSusChem*, 2019, **12**, 2350.
- 115 B. Maji, A. Bhandari, D. Bhattacharya and J. Choudhury, Reusable Single Homogeneous Ir(III)-NHC Catalysts for Bidirectional Hydrogenation–Dehydrogenation of N-Heteroarenes in Water, *Organometallics*, 2022, **41**, 1609.
- 116 B. Maji and J. Choudhury, Switchable Hydrogenation with a Betaine-Derived Bifunctional Ir–NHC Catalyst, *Chem. Commun.*, 2019, **55**, 4574.
- 117 P. Sánchez, M. Hernández-Juárez, N. Rendón, J. López-Serrano, L. L. Santos, E. Álvarez, M. Paneque and A. Suárez, Hydrogenation/Dehydrogenation of N-Heterocycles Catalyzed by Ruthenium Complexes Based on Multimodal Proton-Responsive CNN(H) Pincer Ligands, *Dalton Trans.*, 2020, **49**, 9583.
- 118 S. Chakraborty, W. W. Brennessel and W. D. Jones, A Molecular Iron Catalyst for the Acceptorless Dehydrogenation and Hydrogenation of N-Heterocycles, *J. Am. Chem. Soc.*, 2014, **136**, 8564.
- 119 R. Xu, S. Chakraborty, H. Yuan and W. D. Jones, Acceptorless, Reversible Dehydrogenation and Hydrogenation of N-Heterocycles with a Cobalt Pincer Catalyst, *ACS Catal.*, 2015, **5**, 6350.
- 120 P. Dahiya, N. Garg, R. Poli and B. Sundararaju, Hydrogenation and Dehydrogenation of N-Heterocycles under Cp\*Co(III) Catalysis, *Dalton Trans.*, 2023, **52**, 14752.
- 121 J. Wu, D. Talwar, S. Johnston, M. Yan and J. Xiao, Acceptorless Dehydrogenation of Nitrogen Heterocycles with a Versatile Iridium Catalyst, *Angew. Chem.*, 2013, **125**, 7121.
- 122 W. Yao, Y. Zhang, X. Jia and Z. Huang, Selective Catalytic Transfer Dehydrogenation of Alkanes and Heterocycles by an Iridium Pincer Complex, *Angew. Chem., Int. Ed.*, 2014, **53**, 1390.
- 123 J. Jeong, T. Shimbayashi and K. Fujita, Effect of a Substituent in Cyclopentadienyl Ligand on Iridium-Catalyzed Acceptorless Dehydrogenation of Alcohols and 2-Methyl-1,2,3,4-Tetrahydroquinoline, *Catalysts*, 2019, **9**, 846.
- 124 Y. Wang, L. Qian, Z. Huang, G. Liu and Z. Huang, NCP-type Pincer Iridium Complexes Catalyzed Transfer-Dehydrogenation of Alkanes and Heterocycles, *Chin. J. Chem.*, 2020, **38**, 837.
- 125 S. Muthaiah and S. H. Hong, Acceptorless and Base-Free Dehydrogenation of Alcohols and Amines Using Ruthenium-Hydride Complexes, *Adv. Synth. Catal.*, 2012, **354**, 3045.
- 126 A. E. Wendlandt and S. S. Stahl, Modular o-Quinone Catalyst System for Dehydrogenation of Tetrahydroquinolines under Ambient Conditions, *J. Am. Chem. Soc.*, 2014, **136**, 11910.
- 127 Q. Wang, H. Chai and Z. Yu, Acceptorless Dehydrogenation of N-Heterocycles and Secondary Alcohols by Ru(II)-NNC Complexes Bearing a Pyrazoyl-Indolyl-Pyridine Ligand, *Organometallics*, 2018, **37**, 584.
- 128 D. Manikpuri, D. R. Pradhan, B. Chatterjee and C. Gunanathan, Ruthenium-Catalyzed Acceptorless Dehydrogenation of Heterocycles, *J. Chem. Sci.*, 2022, **134**, 112.
- 129 Y. Wang, C. Li and J. Huang, External-Ligand-Free Aerobic Oxidation of N- and C-Containing Cyclic Systems under Pd-Catalyzed Conditions, *Asian J. Org. Chem.*, 2017, **6**, 44.
- 130 H. Yoo, Y. Yang, S. L. Kim, S. H. Son, Y. H. Jang, J. Shin and N. Kim, Syntheses of 1-H-Indoles, Quinolines, and 6-Membered Aromatic N-Heterocycle-Fused Scaffolds via Palladium(II)-Catalyzed Aerobic Dehydrogenation under Alkoxide-Free Conditions, *Chem. – Asian J.*, 2021, **16**, 3469.
- 131 D. Jung, M. H. Kim and J. Kim, Cu-Catalyzed Aerobic Oxidation of Di-Tert-Butyl Hydrazodicarboxylate to Di-Tert-Butyl Azodicarboxylate and Its Application on Dehydrogenation of 1,2,3,4-Tetrahydroquinolines under Mild Conditions, *Org. Lett.*, 2016, **18**, 6300.
- 132 Y. Shen, F. Chen, Z. Du, H. Zhang, J. Liu and N. Liu, Cu(I) Complexes Catalyzed the Dehydrogenation of N-Heterocycles, *J. Org. Chem.*, 2024, **89**, 4530.
- 133 N. Zumbärgel, M. Sako, S. Takizawa, H. Sasai and H. Gröger, Vanadium-Catalyzed Dehydrogenation of N-Heterocycles in Water, *Org. Lett.*, 2018, **20**, 4723.
- 134 S. Bera, A. Bera and D. Banerjee, Nickel-Catalyzed Dehydrogenation of N-Heterocycles Using Molecular Oxygen, *Org. Lett.*, 2020, **22**, 6458.
- 135 A. Ali and M. N. Shaikh, Recent Developments in Catalyst Design for Liquid Organic Hydrogen Carriers: Bridging the Gap to Affordable Hydrogen Storage, *Int. J. Hydrogen Energy*, 2024, **78**, 1.
- 136 D. F. Brayton and C. M. Jensen, Solvent Free Selective Dehydrogenation of Indolic and Carbazolic Molecules with an Iridium Pincer Catalyst, *Chem. Commun.*, 2014, **50**, 5987.
- 137 P. Rao and M. Yoon, Potential Liquid-Organic Hydrogen Carrier (LOHC) Systems: A Review on Recent Progress, *Energies*, 2020, **13**, 6040.
- 138 S. A. Stepanenko, D. M. Shvitsov, A. P. Koskin, I. P. Koskin, R. G. Kukushkin, P. M. Yeletsky and V. A. Yakovlev, N-Heterocyclic Molecules as Potential Liquid Organic Hydrogen Carriers: Reaction Routes and Dehydrogenation Efficacy, *Catalysts*, 2022, **12**, 1260.
- 139 A. Sogaard, M. Scheuermeyer, A. Bösmann, P. Wasserscheid and A. Riisager, Homogeneously-Catalysed Hydrogen Release/Storage Using the 2-Methylindole/2-Methylindoline LOHC System in Molten Salt-Organic Biphasic Reaction Systems, *Chem. Commun.*, 2019, **55**, 2046.
- 140 L. Li, M. Yang, Y. Dong, P. Mei and H. Cheng, Hydrogen Storage and Release from a New Promising Liquid Organic Hydrogen Storage Carrier (LOHC): 2-Methylindole, *Int. J. Hydrogen Energy*, 2016, **41**, 16129.



- 141 D.-S. Wang, Q.-A. Chen, W. Li, C.-B. Yu, Y.-G. Zhou and X. Zhang, Pd-Catalyzed Asymmetric Hydrogenation of Unprotected Indoles Activated by Brønsted Acids, *J. Am. Chem. Soc.*, 2010, **132**, 8909.
- 142 R. Kuwano, K. Sato, T. Kurokawa, D. Karube and Y. Ito, Catalytic Asymmetric Hydrogenation of Heteroaromatic Compounds, Indoles, *J. Am. Chem. Soc.*, 2000, **122**, 7614.
- 143 R. Kuwano, K. Kaneda, T. Ito, K. Sato, T. Kurokawa and Y. Ito, Highly Enantioselective Synthesis of Chiral 3-Substituted Indolines by Catalytic Asymmetric Hydrogenation of Indoles, *Org. Lett.*, 2004, **6**, 2213.
- 144 R. Kuwano, M. Kashiwabara, K. Sato, T. Ito, K. Kaneda and Y. Ito, Catalytic Asymmetric Hydrogenation of Indoles Using a Rhodium Complex with a Chiral Bisphosphine Ligand PhTRAP, *Tetrahedron: Asymmetry*, 2006, **17**, 521.
- 145 A. Baeza and A. Pfaltz, Iridium-Catalyzed Asymmetric Hydrogenation of N-Protected Indoles, *Chem. – Eur. J.*, 2010, **16**, 2036.
- 146 J. L. Núñez-Rico, H. Fernández-Pérez and A. Vidal-Ferran, Asymmetric Hydrogenation of Unprotected Indoles Using Iridium Complexes Derived from P-OP Ligands and (Reusable) Brønsted Acids, *Green Chem.*, 2014, **16**, 1153.
- 147 J. Wen, X. Fan, R. Tan, H.-C. Chien, Q. Zhou, L. W. Chung and X. Zhang, Brønsted-Acid-Promoted Rh-Catalyzed Asymmetric Hydrogenation of N-Unprotected Indoles: A Cocatalysis of Transition Metal and Anion Binding, *Org. Lett.*, 2018, **20**, 2143.
- 148 Z. Wang, J. Belli and C. M. Jensen, Homogeneous Dehydrogenation of Liquid Organic Hydrogen Carriers Catalyzed by an Iridium PCP Complex, *Faraday Discuss.*, 2011, **151**, 297.
- 149 T. Zhang, Y. Lv, Z. Zhang, Z. Jia and T.-P. Loh, A Rare Earth Metal Catalyzed Aerobic Dehydrogenation of N-Heterocycles, *Org. Lett.*, 2023, **25**, 4468.
- 150 D. Kawauchi, K. Noda, Y. Komatsu, K. Yoshida, H. Ueda and H. Tokuyama, Aerobic Dehydrogenation of N-Heterocycles with Grubbs Catalyst: Its Application to Assisted-Tandem Catalysis to Construct N-Containing Fused Heteroarenes, *Chem. – Eur. J.*, 2020, **26**, 15793.
- 151 M. A. Esteruelas, V. Lezáun, A. Martínez, M. Oliván and E. Oñate, Osmium Hydride Acetylacetonate Complexes and Their Application in Acceptorless Dehydrogenative Coupling of Alcohols and Amines and for the Dehydrogenation of Cyclic Amines, *Organometallics*, 2017, **36**, 2996.
- 152 V. Zubar, J. C. Borghs and M. Rueping, Hydrogenation or Dehydrogenation of N-Containing Heterocycles Catalyzed by a Single Manganese Complex, *Org. Lett.*, 2020, **22**, 3974.
- 153 K. Fujita, Y. Tanaka, M. Kobayashi and R. Yamaguchi, Homogeneous Perdehydrogenation and Perhydrogenation of Fused Bicyclic N-Heterocycles Catalyzed by Iridium Complexes Bearing a Functional Bipyridonate Ligand, *J. Am. Chem. Soc.*, 2014, **136**, 4829.
- 154 K. Fujita, T. Wada and T. Shiraishi, Reversible Interconversion between 2,5-Dimethylpyrazine and 2,5-Dimethylpiperazine by Iridium-Catalyzed Hydrogenation/Dehydrogenation for Efficient Hydrogen Storage, *Angew. Chem., Int. Ed.*, 2017, **56**, 10886.
- 155 D. Teichmann, K. Stark, K. Müller, G. Zöttl, P. Wasserscheid and W. Arlt, Energy storage in residential and commercial buildings via Liquid Organic Hydrogen Carriers (LOHC), *Energy Environ. Sci.*, 2012, **5**, 9044.
- 156 W. Peters, M. Eypasch, T. Frank, J. Schwerdtfeger, C. Körner, A. Bösmanna and P. Wasserscheid, Efficient hydrogen release from perhydro-N-ethylcarbazole using catalyst-coated metallic structures produced by selective electron beam melting, *Energy Environ. Sci.*, 2015, **8**, 641.
- 157 P. Preuster, C. Papp and P. Wasserscheid, Liquid Organic Hydrogen Carriers (LOHCs): Toward a Hydrogen-free Hydrogen Economy, *Acc. Chem. Res.*, 2017, **50**, 74.
- 158 R. H. Morris, Brønsted–Lowry Acid Strength of Metal Hydride and Dihydrogen Complexes, *Chem. Rev.*, 2016, **116**, 8588.
- 159 R. H. Crabtree, Homogeneous Transition Metal Catalysis of Acceptorless Dehydrogenative Alcohol Oxidation: Applications in Hydrogen Storage and to Heterocycle Synthesis, *Chem. Rev.*, 2017, **117**, 9228.
- 160 M. Grasemann and G. Laurenczy, Formic acid as a hydrogen source – recent developments and future trends, *Energy Environ. Sci.*, 2012, **5**, 8171.
- 161 D. Jankovič, M. Mihelač, Ž. Testen, B. Likozar, M. Huš and M. Gazvoda, Mechanistically Guided Development of Homogenous Nickel Catalysis through Rapid Computational Catalyst Screening, *J. Catal.*, 2024, **429**, 115265.
- 162 K. Wu and A. G. Doyle, Parameterization of Phosphine Ligands Demonstrates Enhancement of Nickel Catalysis via Remote Steric Effects, *Nat. Chem.*, 2017, **9**, 779.
- 163 B. Cornils and W. A. Herrmann, Concepts in Homogeneous Catalysis: The Industrial View, *J. Catal.*, 2003, **216**, 23.
- 164 A. Bösmann, G. Franciò, E. Janssen, M. Solinas, W. Leitner and P. Wasserscheid, Activation, Tuning, and Immobilization of Homogeneous Catalysts in an Ionic Liquid/Compressed CO<sub>2</sub> Continuous-Flow System, *Angew. Chem., Int. Ed.*, 2001, **40**, 2697.
- 165 W. Yang, G. A. Filonenko and E. A. Pidko, Performance of Homogeneous Catalysts Viewed in Dynamics, *Chem. Commun.*, 2023, **59**, 1757.
- 166 G. J. Sunley and D. J. Watson, High Productivity Methanol Carbonylation Catalysis Using Iridium. The Cativa™ Process for the Manufacture of Acetic Acid, *Catal. Today*, 2000, **58**, 293.
- 167 M. J. Howard, G. J. Sunley, A. D. Poole, R. J. Watt and B. K. Sharma, New Acetyls Technologies from BP Chemicals, In *Studies in Surface Science and Catalysis*, Elsevier, 1999, vol. 121, pp. 61–68.
- 168 M. J. Howard, M. D. Jones, M. S. Roberts and S. A. Taylor, C1 to Acetyls: Catalysis and Process, *Catal. Today*, 1993, **18**, 325.
- 169 A. E. Lubaev, C. C. Marvin, A. W. Dombrowski and Z. Qureshi, Suzuki–Miyaura Cross-Coupling of Unprotected



- Ortho-Bromoanilines with Benzyl, Alkyl, Aryl, Alkenyl and Heteroaromatic Boronic Esters, *RSC Adv.*, 2024, **14**, 29184.
- 170 N. Miyaura and K. Yamada, A New Stereospecific Cross-Coupling by the Palladium-Catalyzed Reaction of 1-Alkenylboranes with 1-Alkenyl or L-Alkynyl Halides, *Tetrahedron Lett.*, 1979, **36**, 3437.
- 171 S. E. Hooshmand, B. Heidari, R. Sedghi and R. S. Varma, Recent Advances in the Suzuki–Miyaura Cross-Coupling Reaction Using Efficient Catalysts in Eco-Friendly Media, *Green Chem.*, 2019, **21**, 381.
- 172 T. E. Barder and S. L. Buchwald, Insights into Amine Binding to Biaryl Phosphine Palladium Oxidative Addition Complexes and Reductive Elimination from Biaryl Phosphine Aryl palladium Amido Complexes via Density Functional Theory, *J. Am. Chem. Soc.*, 2007, **129**, 12003.
- 173 A. K. King, A. Brar, G. Li and M. Findlater, Homogeneous and Recyclable Palladium Catalysts: Application in Suzuki–Miyaura Cross-Coupling Reactions, *Organometallics*, 2023, **42**, 2353.
- 174 Y.-K. Jeon, J.-Y. Lee, S.-E. Kim and W.-S. Kim, Highly Selective Room-Temperature Suzuki–Miyaura Coupling of Bromo-2-Sulfonyloxy pyridines for Unsymmetrical Diarylpyridines, *J. Org. Chem.*, 2020, **85**, 7399.
- 175 M. J. H. Russell, Water Soluble Rhodium Catalysts. A Hydroformylation System for the Manufacture of Aldehydes for the Fine Chemicals Market, *Platinum Met. Rev.*, 1988, **32**, 179.
- 176 G. D. Frey, 75 Years of Oxo Synthesis – The Success Story of a Discovery at the OXEA Site Ruhrchemie, *J. Organomet. Chem.*, 2014, **754**, 5.
- 177 G. G. Stanley, Hydroformylation (OXO) catalysis, *Kirk-Othmer Encyclopedia of Chemical Technology*, 2000, pp. 1–19.
- 178 B. Cornils and E. G. Kuntz, Introducing TPPTS and Related Ligands for Industrial Biphasic Processes, *J. Organomet. Chem.*, 1995, **502**, 177.
- 179 C. Crause, L. Bennie, L. Damoense, C. L. Dwyer, C. Grove, N. Grimmer, W. J. van Rensburg, M. M. Kirk, K. M. Mokheseng, S. Otto and P. J. Steynberg, Bicyclic Phosphines as Ligands for Cobalt-Catalysed Hydroformylation, *Dalton Trans.*, 2003, **10**, 2036.
- 180 D. M. Hood, R. A. Johnson, A. E. Carpenter, J. M. Younker, D. J. Vinyard and G. G. Stanley, Highly Active Cationic Cobalt(II) Hydroformylation Catalysts, *Science*, 2020, **548**, 542.
- 181 D. M. Hood, R. A. Johnson, D. J. Vinyard, F. R. Fronczek and G. G. Stanley, Cationic Cobalt(II) Bisphosphine Hydroformylation Catalysis: In Situ Spectroscopic and Reaction Studies, *J. Am. Chem. Soc.*, 2023, **145**, 19715.
- 182 T. A. Fassbach, J.-M. Ji, A. J. Vorholt and W. Leitner, Recycling of Homogeneous Catalysts–Basic Principles, Industrial Practice, and Guidelines for Experiments and Evaluation, *ACS Catal.*, 2024, **14**, 7289.
- 183 M. Emura and H. A. Matsuda, Green and Sustainable Approach: Celebrating the 30th Anniversary of the Asymmetric l-Menthol Process, *Chem. Biodiversity*, 2014, **11**, 1688.
- 184 J. H. Jones, The Cativa™ process for the manufacture of acetic acid, *Platinum Met. Rev.*, 2000, **44**, 94.
- 185 V. Fábos, L. T. Mika and I. T. Horváth, Selective Conversion of Levulinic and Formic Acids to  $\gamma$ -Valerolactone with the Shvo Catalyst, *Organometallics*, 2014, **33**, 181.
- 186 F. Valentini, G. Brufani, B. Di Erasmo and L. Vaccaro,  $\gamma$ -Valerolactone (GVL) as a Green and Efficient Dipolar Aprotic Reaction Medium, *Curr. Opin. Green Sustainable Chem.*, 2022, **36**, 100634.
- 187 G. Amenuvor, J. Darkwa and B. C. Makhubela, Homogeneous Polymetallic Ruthenium(II)/Zinc(II) Complexes: Robust Catalysts for the Efficient Hydrogenation of Levulinic Acid to  $\gamma$ -valerolactone, *Catal. Sci. Technol.*, 2018, **8**, 2370.
- 188 A. A. Kiss, Novel Catalytic Reactive Distillation Processes for a Sustainable Chemical Industry, *Top. Catal.*, 2019, **62**, 1132.
- 189 G. J. Harmsen, Reactive Distillation: The Front-Runner of Industrial Process Intensification, *Chem. Eng. Process.*, 2007, **46**, 774.
- 190 R. Muthia, A. G. T. Reijneveld, A. G. J. Van Der Ham, A. J. B. Ten Kate, G. Bargeman, S. R. A. Kersten and A. A. Kiss, Novel Method for Mapping the Applicability of Reactive Distillation, *Chem. Eng. Process.*, 2018, **128**, 263.
- 191 B. Cornils, W. A. Herrmann and R. W. Eckl, Industrial Aspects of Aqueous Catalysis, *J. Mol. Catal. A:Chem.*, 1997, **116**, 27.
- 192 B. Miehlich, A. Savin, H. Stoll and H. Preuss, Results Obtained with the Correlation Energy Density Functionals of Becke and Lee, Yang and Parr, *Chem. Phys. Lett.*, 1989, **157**, 200.
- 193 H. Bahrmann, K. Bergrath, H.-J. Kleiner, P. Lappe, C. Naumann, D. Peters and D. Regnat, BINAS-Synthesis and Use of a New Ligand for Propylene Hydroformylation, *J. Organomet. Chem.*, 1996, **520**, 97.
- 194 H. Mao, H. Yu, J. Chen and X. Liao, Biphasic Catalysis Using Amphiphilic Polyphenols-Chelated Noble Metals as Highly Active and Selective Catalysts, *Sci. Rep.*, 2013, **3**, 2226.
- 195 F. Joó, Biphasic Catalysis–Homogeneous, In *Encyclopedia of Catalysis*, ed. I. Horváth, Wiley, 2010.
- 196 H. Olivier-Bourbigou and F. Hugues, Applications of Ionic Liquids to Biphasic Catalysis, In *Green Industrial Applications of Ionic Liquids*, ed. R. D. Rogers, K. R. Seddon and S. Volkov, Springer Netherlands, Dordrecht, 2003, pp. 67–84.
- 197 T. J. Geldbach and P. J. A. Dyson, Versatile Ruthenium Precursor for Biphasic Catalysis and Its Application in Ionic Liquid Biphasic Transfer Hydrogenation: Conventional vs Task-Specific Catalysts, *J. Am. Chem. Soc.*, 2004, **126**, 8114.
- 198 Q. Chu, M. S. Yu and D. P. Curran, New Fluorous/Organic Biphasic Systems Achieved by Solvent Tuning, *Tetrahedron*, 2007, **63**, 9890.
- 199 A. P. Dobbs and M. R. Kimberley, Fluorous Phase Chemistry: A New Industrial Technology, *J. Fluorine Chem.*, 2002, **118**, 3.



- 200 W. Keim, Oligomerization of Ethylene to  $\alpha$ -Olefins: Discovery and Development of the Shell Higher Olefin Process (SHOP), *Angew. Chem., Int. Ed.*, 2013, **52**, 12492.
- 201 J. Dreimann, A. Vorholt, M. Skiborowski and A. Behr, Removal of Homogeneous Precious Metal Catalysts via Organic Solvent Nanofiltration, *Chem. Eng. Trans.*, 2016, **47**, 343.
- 202 J. Scarpello, The Separation of Homogeneous Organometallic Catalysts Using Solvent-Resistant Nanofiltration, *J. Membr. Sci.*, 2002, **203**, 71.
- 203 M. Janssen, J. Wiltig, C. Müller and D. Vogt, Continuous Rhodium-Catalyzed Hydroformylation of 1-Octene with Polyhedral Oligomeric Silsesquioxanes (POSS) Enlarged Triphenylphosphine, *Angew. Chem.*, 2010, **122**, 7904.
- 204 A. V. Volkov, G. A. Korneeva and G. F. Tereshchenko, Organic Solvent Nanofiltration: Prospects and Application, *Russ. Chem. Rev.*, 2008, **77**, 983.
- 205 S. K. Lim, K. Goh, T.-H. Bae and R. Wang, Polymer-Based Membranes for Solvent-Resistant Nanofiltration: A Review, *Chin. J. Chem. Eng.*, 2017, **25**, 1653.
- 206 F. Xu, S. Zhao, J. Song, Y. Peng and B. Su, Organic Solvent Nanofiltration Membrane with In Situ Constructed Covalent Organic Frameworks as Separation Layer, *Membranes*, 2024, **14**, 234.
- 207 J.-K. Schnoor, M. Fuchs, A. Böcking, M. Wessling and M. A. Liauw, Homogeneous Catalyst Recycling and Separation of a Multicomponent Mixture Using Organic Solvent Nanofiltration, *Chem. Eng. Technol.*, 2019, **42**, 2187.
- 208 R. P. Lively and D. S. Sholl, From Water to Organics in Membrane Separations, *Nat. Mater.*, 2017, **16**, 276.
- 209 J. Geens, A. Hillen, B. Bettens, B. Van Der Bruggen and C. Vandecasteele, Solute Transport in Non-aqueous Nanofiltration: Effect of Membrane Material, *J. Chem. Technol. Biotechnol.*, 2005, **80**, 1371.
- 210 J. A. Whu, B. C. Baltzis and K. K. Sirkar, Nanofiltration Studies of Larger Organic Microsolutes in Methanol Solutions, *J. Membr. Sci.*, 2000, **170**, 159.
- 211 P. Schmidt and P. Lutze, Characterisation of Organic Solvent Nanofiltration Membranes in Multi-Component Mixtures: Phenomena-Based Modelling and Membrane Modelling Maps, *J. Membr. Sci.*, 2013, **445**, 183.
- 212 R. M. Gould, L. S. White and C. R. Wildemuth, Membrane Separation in Solvent Lube Dewaxing, *Environ. Prog.*, 2001, **20**, 12.
- 213 J.-K. Schnoor, J. Bettmer, J. Kamp, M. Wessling and M. A. Liauw, Recycling and Separation of Homogeneous Catalyst from Aqueous Multicomponent Mixture by Organic Solvent Nanofiltration, *Membranes*, 2021, **11**, 423.
- 214 Z. Wen, D. Pintossi, M. Nuño and T. Noël, Membrane-Based TBADT Recovery as a Strategy to Increase the Sustainability of Continuous-Flow Photocatalytic HAT Transformations, *Nat. Commun.*, 2022, **13**, 6147.
- 215 T. Aca Bayrakdar, F. Nahra, D. Ormerod and S. P. Nolan, Integrating Membrane Separation with Gold-catalyzed Carboxylative Cyclization of Propargylamine and Catalyst Recovery via Organic Solvent Nanofiltration, *J. Chem. Technol. Biotechnol.*, 2021, **96**, 3371.

